The Application of Carbon Furnace
Atomisation to the Determination
of Indium in Galena and Sphalerite

by

David Archibald Banks

Department of Pure and Applied Chemistry
University of Strathclyde, Glasgow

A thesis submitted in part fulfillment of the requirement for the degree of Master of Science.

June 1982

Acknowledgements

I wish to express my gratitude to J. M. Ottaway for providing the facilities at Strathclyde University and for his unselfish guidance and assistance during the course of this research.

I also wish to express my thanks to the British Steel Corporation for their financial support and provision of facilities at Ravenscraig Steelworks. My gratitude is especially extended to Mr Andrew Cunningham, the laboratory manager, and to Mr David Lambie whose many ideas and encouragement were invaluable.

SUMMARY

The work described in this thesis involved the application of electrothermal atomisation, allied to atomic absorption and atomic emission spectrometry, to the determination of indium in the lead and zinc ores, galena and sphalerite. Samples of the ores were collected from sites in Scotland, Northern England and Eire.

Optimum conditions were established for different types of tube and platform atomisers and the detection limits compared for each. The detection limits ranged from 1 to 3 $\mu g l^{-1}$ for atomic absorption and from 0.08 to 1.0 $\mu g\, l^{-1}$ for atomic emission. The effect of various acids and metal ions on the indium signal was determined and possible interferences identified.

A simple method based on dissolution of 1g samples of galena in nitric acid followed by addition of sulphuric acid proved satisfactory. For sphalerite determinations, 0.5g samples were dissolved in nitric acid.

Comparison of the analytical results obtained by atomic absorption and emission was carried out and the two methods were shown to yield good agreement.

CONTENTS

INTRODUCTION

Unlike their predecessors modern geologists are becoming more aware of the benefits which can be derived from the detection, in a variety of materials, of certain elements at the part per million level or below. Twenty one elements, omitting the rare gases and short lived radioactive elements, have crustal abundances, which are sub parts per million. From work carried out in recent years, it has become evident that it is the trace element distribution which will point the way forward in the elucidation of many complex geological problems. Trace elements of particular interest to igneous petrologists include Rb,Ba,Sr,Zr,Y,Nb,Th, the rare earth elements La to Lu, Ni,V and Cr. Different minerals may incorporate or exclude trace elements with a greater selectivity than they do major elements and these preferences exert such a critical influence on the distribution that their analysis can lead to constraints on the nature and composition of mineral assemblages with which the magma may have been previously equilibrated. Economic geology has also derived great benefits from trace element analysis in that the processes and sources responsible for ore deposits may be more clearly defined. This greater understanding leads in turn to the location of possible sites of deposition and often in actual discoveries. Analysis of the manganese concentrations[1] in certain limestones has shown a distinct enrichment near exhalative sulphide orebodies. Analysis of plants and vegetation has shown the presence of some molybdenum ore deposits.

This interest in trace analysis has been aroused mainly due to the development of modern instrumental methods of analysis which are capable of rapid and accurate determinations of the trace constituents of rocks. X-ray fluorescence, atomic absorption,neutron activation, mass spectrometric isotope dilution and other analytical procedures have provided the geologist with the means for accurate low level analysis for which applications are still being found.

The research studies described in this particular thesis have been concerned with one particular trace element, indium, and its determination in the lead and zinc ores galena and sphalerite. The distribution of this element appears to be dependant on the temperature of deposition of the sphalerite, which attracts the major portion of available indium, leaving only minor quantities in galena. Little work has been carried out on this element as previously the methods available lacked sufficient sensitivity for low level determinations.

One of the early methods of determination was gravimetry as the phosphate, but to gain enough precipitate for a reasonably accurate determination 100g of sample was required. Neutron activation is one of the more popular modern trace analysis methods[2,3]. However, when irradiation of complex materials such as rocks and ores takes place the activity induced is composed of a great number of radionuclides. Often complicated separation techniques are required to obtain satisfactory radiochemical purity of the final product. Another method widely employed is to use the emission spectra produced by a d.c. arc in which the sample is placed in a graphite electrode[4,5]. The sample may either be placed directly into the electrode or may be disssolved, the indium extracted and then arced. The emission spectra are generally recorded on photographic plates and the density of the spectral lines subsequently measured. Other methods used in the determination of indium include mass spectrometry[6], polarography[7], and colorimetry[8].

CHAPTER ONE

INDIUM

1.1 Production and Uses

Indium was first discovered in 1863 by F. Reich and T. Richter during the examination of a Freiberg sphalerite. Traces of thallium were being sought for but the spectroscope failed to show the green thallium line, revealing instead an indigo-blue line which had never before been observed. A new element was extracted and named indium from this prominent spectral line. Indium has been observed in the atmosphere of the sun and has been found in meteorites. The cosmic abundance derived from analysis of meteorites has been estimated at 0.5μg/g and the crustal abundance estimated at 0.11μg/g.

The main source of indium is from zinc ores and to a lesser extent from ores of lead, copper and iron. The indium is obtained as a by-product of zinc smelting with the indium being leached from the crude zinc liquors by acid followed either by precipitation as phosphate or by precipitation on metallic zinc rods. Until 1924 about one gram constituted the worlds supply of the element in its isolated form but in 1976 annual production had risen to around 48 tons with Japan the free worlds largest producer.

Indium has applications in the making of low melting point alloys, an alloy containing 24% indium and 76% gallium is liquid at room temperature. It is also used in the manufacture of bearing alloys, germanium transistors, rectifiers, thermistors and photoconductors. It can be plated onto metal or evaporated onto glass forming a mirror as good as that obtained with silver but with more resistance to atmospheric corrosion. In medicine, radioisotopes of indium in compounds such as indium trichloride, and colloidal indium hydroxide are used in the treatment of tumors and in organ scanning.

1.2 Geochemistry

When a trace-element such as indium is detected in a mineral it is usually present in one of two situations[9]. Either it is contained in inclusions of another mineral or it must occupy a lattice site in the principal mineral. However it is also possible that the element is held by absorption or other surface effects or is concealed within the mineral in some "cavity" or structural defect. These latter possibilities are unlikely for most elements and can usually be neglected. Trace elements in the minerals are commonly held in a structural position usually occupied by a major element of similar size, valency and chemical properties.

In Table 1.2.1 the ionic radii for trivalent indium and the other elements, in their usual valency states in rocks, lying within ± 15% of that value are given. Minerals which contain any of these other metals should be able to carry indium in their place, with two provisos. Firstly the metal being replaced must be chemically similar, especially so far as bonding is concerned. Secondly, another substitution may be necessary to balance the valencies. Among the silicate minerals the only ones which contain detectable amounts of indium are the mafics. The minerals zircon, apatite, lepidolite, titanite and feldspars do not contain detectable amounts of indium. Thus it is doubtful whether the elements Li,Hf,Sr,Na,Lu,Ce,Yb,Ca and Y are vicarious with indium, which is to be expected as they are chemically very different to indium. Goldschmidt[10] concluded that indium follows divalent iron and manganese although very few manganese minerals have been found to contain indium and the replacement of iron does not extend to iron sulphides as recorded by Erametsa[11]. Numerous authors have reported the occurrence of indium in tin and tungsten minerals such as cassiterite, wolframite and scheelite with values ranging from 0.5 to 100μg/g. The tin - indium association would seem to be particularly strong as Ottemann[12] has shown that minerals from the Hartz region which were rich in tin were also relatively rich in indium.

TABLE 1.2.1

Ionic Radii of Metal Ions

Element	Å	Element	Å	Element	Å
Li + 1	0.78	In + 3	0.92	Cu + 1	0.96
Mg + 2	0.78			Na + 1	0.98
Ni + 2	0.78			Lu + 3	0.99
Co + 2	0.83			Ce + 4	1.02
Sc + 3	0.83			Yb + 2	1.03
Fe + 2	0.83			Cd + 2	1.03
Zn + 2	0.83			Ca + 2	1.06
Cu + 2	0.83			Y + 3	1.06
Hf + 4	0.86				
Zr + 4	0.87				
Sb + 3	0.90				
Mn + 2	0.91				

Erametsa established the predominant chalcophile tendancies of indium, showing that in hydrothermal deposits it commonly follows zinc and sometimes copper. Sphalerite samples from Finnish deposits contain on average 100µg/g with some containing as much as 1% indium. In a survey of trace elements from British deposits Shazly[13] found indium values ranging from 20 to 300µg/g in epigenetic sphalerites with an apparent absence in syngenetic deposits. The sphalerites associated with the granite masses of the south west of England display the highest concentrations of indium, the concentration decreasing with increasing distance from the granite mass. From the large number of sphalerite analyses carried out by various workers it is evident that wherever this mineral is forming it will collect all the indium available. The only other minerals showing a fairly consistent indium enrichment are chalcopyrite and chalcocite. These associations are in agreement with the figures in Table 1.2.1, the replacement of zinc by indium in sphalerite probably being accompanied by an equivalent substitution of zinc by copper to balance the valencies. The indium values for silicates are rather erratic but indicate the camouflage or capture of indium by iron. The highest values are to be found in hornblendes and micas which is to be expected as the In(+3) - Fe(+2) replacement requires a second replacement to balance the valencies and these minerals have considerable elasticity in this respect. No indium has been detected in any feldspar samples due mainly to the improbability that an indium feldspar can exist.

The distribution of indium in igneous rocks would appear to be very irregular with no fixed pattern. Basic rocks frequently contain appreciable amounts of the metal but the highest values occur in granites. This does not appear to be in accordance with crystal chemical considerations, if indium is camouflaged in the silicates, but there are two possibilities to explain this. Either the indium is present in the silicates and there exists indium provencies in time or space, or else the indium is contained partly or wholly in some other mineral. To date no valid evidence exists for the first explanation but the second possibility is more likely. Apart from the silicates all the igneous rocks contain varying amounts of iron oxides and sulphides. The former undoubtedly carry some indium, around 0.1µg/g, but iron oxides seldom constitute more than 5% of an igneous rock and so can contribute little to thewhole analysis. On the other hand, the sulphides are usually present in much smaller quantities. The normal magmatic accessory sulphides are pyrite, pyrrhotite and chalcopyrite And of these chalcopyrite probably contributes most of the indium content. As this mineral can contain up to 1000µg/g a small quantity of sulphide may notably increase the whole indium content.

The mean igneous rock contains 0.11µg/g indium and during weathering the indium is commonly transported towards the sea, probably as a colloidal hydroxide suspension. The indium appears to remain in suspension until flocculation takes place when the sea is reached, the precipitated material being incorporated in the argillacious sediments. Some indium must remain in solution since it has been found in marine phosphates of chemical and possibly biological origin, but the quantity in solution is too minute to detect. In addition there is evidence that indium is concentrated slightly by other biological factors since a slightly increased concentration has been observed in some carbonaceous shales and in some coal ash for which up to 2.0µg/g has been reported. This can be attributed to the establishment of a strong reducing environment during the bacterial reduction of dead organic matter, and the consequent incorporation of indium in authigenic sulphides.

1.3 GEOLOGY OF THE SAMPLE LOCALITES

1.3.1 Leadhills and Wanlockhead

The best known metalliferous deposits in Scotland are the epigenetic lead-zinc veins in the Caledonian geosyncline, most notably in the Leadhills - Wanlockhead district of the Southern Uplands, where galena was mined from the seventeenth century until the 1930's and again briefly in 1958. The Southern Uplands represents part of the non-metamorphic complex of the Caledonian geosyncline, which is predominantly eugeosynclinal and where deformation commenced in the late Silurian. Although the important lead-zinc veins of Scotland occupy fissure-fillings in lower Palaeozoic and late Proterozoic rocks of the Caledonides, there is geoligical and isotopic evidence that they were placed in their present position in Carboniferous - Permian times.

The 70 or more known veins of this district occur in Ordovician greywackes that are separated by northwesterly dipping reverse faults[14] from older Ordovician black shales to the northwest. Faulting has produced more open spaces suitable for mineral deposition in the greywackes than in the shales and associated cherts which may in fact have acted as an impervious barrier to the mineralisation. A WNW to NW trending set of veins is possibly older than the main NNW to NNE trending set, the directions of the veins corresponding to the pattern of Caledonian wrench faulting in the Southern Uplands[15]. Steep easterly dips are characteristic of the veins which vary in width from a few centimetres to about 5 metres.

They consist of brecciated greywacke cemented by dolomite and calcite and cut by vertical stringers of galena. Some concentration of sulphides on slickensided vein walls commonly the footwall, has been observed.

One of the largest oreshoots found at Leadhills-Wanlockhead was in the New Glencrieff vein, extending some 360 metres along strike and nearly 400 metres downdip. High-grade pockets of lead ore occurred characteristically at the vein junctions. Production over the period 1842-1958 has been estimated at more than 300,000 tonnes of lead[16] with about 25 tonnes of by-product silver. The region is also of interest because of the large variety of mineral species which are to be found, 57 have been recognised by Temple[17].

Potassium - argon isotopic age determinations have been carried out on clay mineral fractions from the various veins. The ages range from 265 to 343 m.y[18] with the WNW-NW veins showing ages which are slightly older than the NNW-NNE suite.

1.3.2 Tyndrum

The Tyndrum ore deposit of the Central Highlands consists of six parallel veins traversing the schists of the country rock and having a close association with one of the faults of the Tyndrum Fault zone. All the veins except one yielded galena, sphalerite, pyrite and chalcopyrite as the main ores with calcite, barite and quartz as the gangue minerals. The veins have a maximum thickness of 20 feet with the ores occurring in some cases as ribs 2 feet wide. To the north the country rocks are predominantly quartzitic flags while to the south of the major vein deposit mica schists predominate.

As with the Leadhills-Wanlockhead deposit potassium-argon isotopic age determinations have been carried out and these range from 296 to 334 m.y. with a mean of 315my for the deposit.

1.3.3 Silvermines

At Silvermines in County Tipperary[19] lead-zinc mineralisation occurs as syngenetic stratiform orebodies in a limestone sequence, as fault-bounded epigenetic strata-bound orebodies in the basal Carboniferous and structurally controlled vein or breccia zones in the Upper Devonian sandstones. The large stratiform orebody occurs in massive partly brecciated pyrite at the base of a thick sequence of dolomite breccias. The maximum thickness of the ore is 30 metres. At the base there is usually an abrupt change to massive pyrite from a footwall of nodular micrite, shale, biomicrite and other limestone units of the Mudbank Limestone. Sometimes the contact is gradational but the upper contact is always sharp.

Pyrite and marcasite make up 75% of the ore, sphalerite forms 20% and galena 4%. The deposit contains approximately 500,000 tonnes of lead and 1,300,000 tonnes of zinc[20] and ranks as one of the ten largest deposits in the world.

1.3.4 Northern England

The north Pennine orefield has been the most important source of lead in Britain[21] yielding approximately 4 million tons of lead in addition, to considerable quantities of zinc, fluorite, barite and witherite. The earliest records of mining date from the 12th century but it was in the 18th and especially the 19th century that lead mining in the area was particularly active.

The orefield covers an area of 550 square miles and is bounded to the northwest and the south by major faults. The faults have displacements of up to 3000 metres with the major displacements taking place during the Tertiary period. The deposits occur mainly in fissure veins that cut a sequence of Carboniferous sediments composed of alterations of limestone-shale-sandstone. The fractures in which the mineral veins are deposited stand nearly vertical in the sandstones and limestones but assume a considerable dip in the shales. Nearly all the faults and fractures within the orefield exhibit some degree of mineralisation but workable orebodies occur mainly where fractures of small displacement cross competent beds. The form of many of these orebodies is ribbon-like with a length many times greater than their height.

From lead isotope studies of the pennine galenas an age of 280 m.y. has been proposed for the mineralisation.

CHAPTER TWO

ELECTROTHERMAL ATOMISATION

2.1 HISTORY

The first development of electrothermal atomisers can largely be attributed to the work of King[22] during the period 1905 to 1908. His interest during this time was in the observation of emission spectra of atoms and molecules without the complicating factors of electrical conduction in arc and spark spectra and chemical reactions which occur in flame spectra. His aim was to produce emission spectra solely by the use of heat. The first furnace used by King was an arc-heated device with which temperatures of 2200°C could be obtained.

No use, however, was made of the principle of electrothermal atomisation for quantitative analytical measurements until 1956 when two groups of workers[23] in the U.S.S.R. used an electrothermal vaporisation technique to separate and preconcentrate trace elements onto a graphite electrode prior to emission analysis. In 1959 L'vov[24] published his work on the application of electrothermal furnace atomisers for quantitative atomic absorption analysis. The furnace used in his early work was similar in principle to that used by King, consisting of a graphite furnace 100mm in length with an external diameter of 10mm and an internal diameter of 3mm. The furnace was lined with tantalum foil to decrease the loss of atomic vapour by diffusion through the porous carbon. A carbon electrode was used for the sample introduction and an auxiliary electrode for producing a d.c. arc to the sample electrode. The furnace had an aluminium cover which contained two quartz windows used for the atomic absorption measurements. The analysis was carried out by placing 0.1mg of sample on the tip of the sample electrode, four of which could be placed in the apparatus, which was then evacuated and filled with argon. The carbon furnace was preheated to the desired temperature before the sample electrode was moved into the opening in the furnace wall. As the sample entered the furnace the d.c. arc was switched on for 3-4 seconds causing the electrode tip to heat and the sample to vaporise. Heating the sample with the d.c. arc proved to be inefficient and later models used resistive heating for the sample as well as the furnace.

In 1967 the biggest step forward in the development of an electrothermal atomiser which could be used in a routine analytical laboratory with commercially available spectrometers took place. Massmann[25,26] produced a simplified and compact version of the resistively heated King furnace to enable both atomic absorption and fluorescence measurements to be made. The furnace consisted of a graphite tube 55mm in length, 6.5mm internal diameter and 8.0mm external diameter. Liquid samples up to 200μl could be introduced through a 2mm diameter hole at the centre of the tube. The graphite tube was operated in an atmosphere of argon and was supported between two water cooled steel cones which were electrically insulated from each other. This design of furnace became the basis for most of the furnaces used in current commercial instruments.

There are also a large number of miscellaneous atomisers which have been produced over the years, but these were basically for research purposes and did not become commercially available. Examples of these are a furnace, similar to L'vov's produced around 1968 by Woodriff[27] but which was too large to fit into commercial spectrometers and carbon filament atomisers produced in 1969 by West[28] which could be used for both atomic absorption and fluorescence measurements. The development of metal filament atomisers also continued in 1969 with the use of electrically heated platinum or tungsten wire loops and in 1970 an electrically heated tantalum boat was developed by Donega and Burgess[29].

Whilst the original work of King was concerned with the measurement of emission spectra, the present day electrothermal atomisers have utilised the technique of atomic absorption for analytical measurements. However the use of these atomisers to produce emission spectra for quantitative measurements is becoming more popular but is unlikely at present to replace atomic absorption as the preferred technique in routine use.

2.2 Atomisation Processes

The mechanisms by which atoms are released from graphite atomisers has been the subject of several theories[30,31,32]. It would seem that the processes involved in furnace atomisation are simpler than those involved in flame atomisation but various reactions are still possible.

Evaporation of the metal oxide prior to atomisation will occur for some elements whose oxides have a high vapour pressure at temperatures where atomisation is first observed. Significant diminution of the atomic absorption signal would be expected to occur under these conditions and the problem is even more critical where metal chlorides, which are highly volatile, are present in the atomiser. Thermal dissociation of the oxide is another possibility with the liberated oxygen and the furnace carbon playing a role in controlling the degree of dissociation. The mechanism which is relevant for most elements is the reduction of the metal oxide by the furnace according to the equation.

$$M_xO_y(s) + C(s) \leftrightarrow xM(g) + yCO(g)$$

The temperature at which atomic absorption commences is the temperature which is favorable for the reduction of the oxides. The start of this reaction corresponds to the temperature at which the change of the free energy of the reaction $\Delta G^o = o$. Another possibility for some elements is the formation of carbides from the oxides of the elements. From theoretical considerations it can be shown that this would occur at lower temperatures than gaseous atom formation for several elements.

Atom Removal

de Galan[33,34] has shown that the atom removal function is much more rapid than the supply function under normal conditions. In furnaces with gas flow, the removal of atoms takes place in about 0.1 seconds, although in larger furnaces with gas stop conditions the time for removal is extended to about 1 second which is approximately the same as the supply time. Many authors assume that the rate of removal of atoms is proportional to the number present in the system. This however is not the case as there are several factors which render the supposed relationship incorrect.

The contact between the analyte and the furnace only takes place with a small part of the centre of the tube. Initially a constant response occurs but this decays exponentially as diffusion occurs towards the ends. The atomisation of the analyte takes place while the temperature of the furnace is still increasing and atoms are therefore expelled along with the expanding gases of the furnace. This effect is especially relevant in open-ended types of atomisers. Atomisation under gas flow conditions causes convective removal of the analyte element as well as enhancing the expansion effect. This is reduced by operating the furnace under reduced flow or gas stop conditions. Diffusion of the atomic vapour also takes place through porous walls of the carbon furnace and there is some evidence that diffusion through the walls may be greater than from the open ends of the tube.

2.3 Mathematical Model for a HGA74 Furnace

There are basically two kinetic models which can be used to describe the atomisation process. L'vov[35] describes a process where atomisation takes place under increasing temperature and Fuller[36] uses a model where atomisation is assumed to take place under isothermal conditions. Neither of these models is completely satisfactory with both theories having advantages. L'vov's model approximates the situation for easily atomised elements at high temperatures in a furnace and Fuller's model approaches the situation existing in a furnace particularly for elements which are difficult to atomise and at low temperatures.

Akman[37] has proposed a mathematical model for the atom formation and dissipation mechanisms in a HGA74 furnace which attempts to fit the experimentally derived absorption profile to a calculated profile.

The concentration of atoms in the furnace at any given time can be expressed by the equation

$$\frac{dN}{dt} = n_1(t) - n_2(t) \qquad \ldots\ldots\ldots \quad (1)$$

Where $n_1(t)$ is the number of atoms entering the analytical volume and $n_2(t)$ is the number of atoms leaving the system per unit time. Three assumptions are made (a) All the atoms remain in the system until the start of the signal and therefore $n_2(t)$ can be neglected, (b) Complete atomisation of the sample takes place during the period from the beginning of atomisation to the point of maximum signal and (c) Atomisation takes place under constantly increasing temperature, and so approximates to L'vov's model. Atom formation in the furnace can then be described by the following two equations

$$n_1(t) = \frac{dN}{dt} \simeq At \quad .... \qquad (2)$$

and

$$n_1(t) = \frac{2N_o}{T_1^2} t \quad .... \qquad (3)$$

Where N_o is the number of atoms in the system and T_1 the atomisation period up to the point of maximum signal. The signals derived from this theory are exactly the same as those obtained experimentally at the beginning of the atomisation period. During later stages atom loss and gas-phase reactions occur and this simple theory breaks down. The supply of analyte cannot however be described completely by a first order rate constant with an Arrhenius-type temperature dependence.

The atom removal function can be approximated by an exponential decay

$$n_2(t) = k_2N \quad .... \qquad (4)$$

and when account is taken of the atoms remaining in the furnace during atom formation, the rate of furnace heating and the physiochemical properties (B) of individual elements equation (1) can be modified to give:

$$\frac{dN}{dt} = B(N_o - N)t - k_2N \quad .... \qquad (5)$$

If a previous assumption that atoms are not removed from the system at the very beginning then equation (5) yields on integration:

$$N = \frac{BN_0t^2}{2} \quad \ldots\ldots\ldots\ldots \quad (6)$$

Akman[38] has shown that the number of atoms which are unatomised can be expressed by:

$$N = pA \quad \ldots\ldots\ldots\ldots \quad (7)$$

which on substitution in equation (6) yields:

$$A = \frac{BN_0t^2}{2p} \quad \ldots\ldots\ldots\ldots \quad (8)$$

Here A is the absorbance at any time and p is a proportionality constant relating the amount of vapour in the furnace to the absorbance and is constant with temperature.

The production and removal of atoms in this furnace is controlled entirely by the heating program and the physical properties of the analyte element. Where the model breaks down is in the portion of the signal at later stages after the absorbance maximum. Here the term relating to the removal of atoms from the furnace cannot be neglected as this term becomes more effective towards the end of the signal. Thus the correct solution for equation (5) should be:

$$N = \frac{BN_0\ t^2}{2} - \frac{k_2BN_0\ t^3}{6} - \frac{BN_0\ t^4}{8} \quad \ldots\ldots (9)$$

The heating of the furnace is also non-uniform with a thermal gradient existing along the length of the tube. The atomic vapour from the hotter centre may on outward diffusion condense and be re-evaporated as the hot central zone spreads outwards. The start of gas flow conditions begins after 8 seconds in the HGA74 furnace which will alter the value of k_2, the atom removal rate constant in equation (5).

2.4 PLATFORM ATOMISATION

In an attempt to modify the conditions under which atomisation takes place in commercial atomisers, L'vov[39] suggested the atomisation of the sample from a platform placed inside the graphite tube. The function of this platform is to delay the atomisation of the sample until near isothermal conditions exist within the graphite tube which causes an increase in sensitivity for many elements. Only with long heating times do near isothermal conditions exist in graphite tubes, but as the heating rate of the platform is slower than that of the tube the atomisation is shifted to longer times. Thus the situation with the platform conforms more closely to Fuller's model where atomisation takes place under isothermal conditions.

The rate of heat gain or loss between the tube and the platform is proportional to the difference in temperature of the two bodies. i.e.

$$\frac{dQ}{dt} \propto (T^4 - T_o^4)$$

where T and T_o are the temperatures of the energy emitter and receiver respectively. However as the temperature of the tube is much higher than the platform an approximation may be made by neglecting T_o which means that the heating rate of the platform is proportional to the fourth power of the tube temperature. Because of this relationship it is difficult to insulate the platform from this radiation to achieve a desirable temperature lag. The theory of heat transfer states that if a surface absorbs energy incident upon it, the surface will also emit the same amount of energy incident upon it from within. Any method of making the surface of the tube and platform more reflective would be effective in decreasing the amount of energy emitted by the tube and absorbed by the platform. This type of surface can be obtained by coating the surface of the tube with pyrolytic graphite which produces a much smoother surface.

Heating of the platform is due mainly to the radiational transfer of heat from the hot graphite tube and to a much lesser extent by thermal conduction at the points of physical contact between the graphite tube and the platform surface. In practice this contact may be significantly reduced by removing some of the graphite along the edge of the platform leaving only the four corners of the platform in contact with the tube wall. Increasing the mass of the platform also tends to increase the time required to achieve atomisation of the sample.

The net effect of using platform atomisation is to significantly reduce several factors which lead to the loss of analyte and so reduce sensitivity. The large thermal gradients which normally exist within graphite tubes are reduced giving increased sensitivity as the analyte is no longer condensed at the cooler ends of the atomiser. The expanding inert gas within the graphite tube also causes expulsion of up to 20%[40] of the analyte atoms from the tube. However the delay caused by the platform means that atomisation takes place at a time when the inert gas has expanded to its final volume. Matrix effects for some samples[41] are also reduced with this system leading to improved sensitivities and precision.

2.5 TANTALUM TREATED ATOMISER TUBES

Electrothermal atomisation has become a widespread and popular technique in many analytical laboratories. Atomisation of samples in graphite tubes at temperatures of up to 3000°C make the technique exceptionally sensitive and capable of determining a large number of trace elements in many sample matrices. However the continued use of high temperatures causes deterioration of the tube and variation of the signal response. Various treatments including the in situ coating with pyrolytic graphite have been tried but in these only the interior of the tube is affected and the exterior surface is left unprotected. No substantial improvement is therefore achieved in the tube lifetime.

The tantalum treatment proposed by Zatka[42] produces a thermally protective layer of refractory metal carbide over all of the graphite tube surface. The interstitial carbide formed is thermodynamically stable with a very high melting point of 4270°C and a low vapour pressure. The carbide is electroconductive, chemically inert and increases the life of the tube without altering its physical properties. Initial treatment produces tantalum through the whole thickness of the tube, the second producing a layer only on the surface of the tube.

The reproducibility and sensitivity is substantially improved by the tantalum carbide even after extended use at high temperatures. Normal graphite tubes only last in the region of 60 firings at 2700°C while the treated tubes can survive 350-400 firings at this temperature with no real significant loss in sensitivity. These tubes were found to be especially good when dealing with samples containing reasonable amounts of acids which tend to destroy normal tubes.

2.6 INTERFERENCES

Interferences are the major problem associated with the use of electrothermal atomisers as atom cells for use in atomic absorption and atomic emission spectrometry. A review of the literature shows that numerous authors have reported the occurrence of interferences but very few have made an attempt at explaining the root cause of such effects. In this section the various types of interferences will be discussed under the headings of chemical, physical and spectral interferences.

Chemical interferences in electrothermal atomisation are probably best described as volatile compound formation in which the analyte element is wholly or partly lost from the furnace tube before atomisation, or by the formation of stable compounds where atomisation is wholly or partly prevented. Analyte loss during the pyrolysis stage can occur for two reasons: Firstly, the element may be present in the sample in such a form that it is significantly volatile at the pyrolysis temperature, or secondly, it may be converted into a volatile form by the sample matrix. The presence of oxyanions is preferred to halides in the sample matrix as the loss of the analyte element is likely to occur through vaporisation of molecular halide species. If such losses do not occur during the pyrolysis stage then the halides may be lost during the early part of the atomisation cycle when the temperature is still relatively low. Condensation of the analyte element in the cooler regions of the tube is likely to be enhanced by large quantities of other elements in the matrix which are atomised or vaporised at similar temperatures. The slow release of the element in its atomic form is often attributed to the formation of stable carbide species with the tube carbon. The extent and ease of this carbide formation is known to depend on the state of the graphite atomiser surface which should be kept reproducible for all atomisations.

The major physical problems encountered with electrothermal atomisers are often related to the large thermal gradient which exists along the length of the graphite tube. The physical effects of surface tension and viscosity of the solution play a less important role than in flame atomisation, but spreading of the solution within the tube is important especially in the light of the thermal gradient. Spreading will cause variations in the signal response, especially in the peak height signal but may not vary so much with integrated signals. Highly volatile elements may be atomised and then condensed in cooler parts of the tubes but when this heats up atomisation will again take place and double peaks will be observed. Incomplete atomisation of an element causes subsequent enhancement in further analytical determinations with the errors becoming progressively worse. The greatest problem is with elements which form stable refractory oxides and high temperatures are essential to ensure complete atomisation. Large concentrations of matrix during atomisation can cause scattering of the incident light beam and molecular species which are also atomised can cause molecular absorption by their broad band and line spectra. These effects may be overcome by the use of background correction techniques.

Spectral interferences in electrothermal atomisation are basically the same as those encountered in flame atomisation. A serious difference is due to the background species in the flame as compared to those in the furnace. In the flame many different absorbing species can occur but this problem is simplified in the furnace with the use of an inert gas atmosphere. Actual spectral line interference in which two atomic lines overlap or are unresolved is relatively rare in atomic absorption analysis. This type of interference is more common in atomic emission where light is emitted not only by the test element but also by other elements in the sample. If the wavelength of the interfering radiation is close enough to the line of the element being measured, it will not be resolved and will be detected and recorded along with the signal for the element.

2.7 CARBON FURNACE ATOMIC EMISSION

The use of carbon furnaces as an atom source for atomic absorption is now well established as an analytical technique in most laboratories. However, the use of these furnaces to produce atomic spectra suitable for emission measurements is only now becoming more popular. To date more than 40 elements have been determined at sub p.p.m. levels in a variety of matrices.

Compared with more popular emission sources the carbon furnace operates at a relatively low temperature of around 3000°C maximum. This is a distinct advantage in some respects as only simple spectra are obtained but a continuum background is still present due to Rayleigh scattering of the tube wall radiation by atoms and molecules in the vapour phase of the furnace.[43] The temperature of the vapour phase is one of the limitations in achieving lower detection limits as the sensitivity for the determination of the analyte element is exponentially related to the temperature of the vapour during the residence time of the atom population. Platform atomisation as discussed earlier significantly improves detection limits as the analyte element is released into the vapour at a considerably higher temperature.

There are 3 main methods of metal atom excitation in electrically heated graphite atomisers. These are transfer of translational energy from electrons which are in collision with the metal atoms, the transfer of vibrational and rotational energy caused by the collisions with molecules and discrete absorption of radiation from the tube wall continuum. The 3 processes can be shown by the following equations:

$$M + e^- \leftrightarrow M^* + e^-$$

$$M + XY \leftrightarrow M^* + XY$$

$$M + h\nu \leftrightarrow M^*$$

Monatomic species show a low efficiency in the electronic excitation of metal atoms, but because of their much smaller mass and high mean velocity under thermal conditions, they are highly efficient in the reduction of the population of atomic electronic states lying within several electronvolts of the ground state. The concentration of molecular species in the furnace depends on several factors such as temperature, furnace design and the inert gas used. With nitrogen as the inert gas the molecular species in the furnace will be completely dominated by nitrogen molecules, however, with argon as the inert gas the molecular concentration arises from nitrogen and oxygen present as impurities in the argon, desorption from the furnace and contributions from the atmosphere. Molecular carbon species are also present in the furnace but their concentration at the atomisation temperature of most elements is very low. In a nitrogen atmosphere the excitation of atomic and molecular species is about 10^4 times faster than in argon, however the de-excitation process is also faster by the same amount.

In general it is found that electron collisions do not contribute greatly to the excitation process, although their contribution does increase substantially with increased temperature. Photon absorption and more significantly molecular collisions with nitrogen are the processes which contribute most to atom excitation.

As mentioned earlier analyte sensitivity is exponentially related to the vapour temperature. Sturgeon[44] has measured the excitation temperature for the atomic vapour of several elements including indium, for which he suggests the vapour reaches a maximum of 1600K when the wall temperature is 2700K. Several other workers have also achieved this large temperature difference, however many have also found the opposite to be true[45,46] in that the vapour temperature closely matches the wall temperature. Detailed work by Littlejohn[47] clearly shows that in graphite atomisers local thermal equilibrium exists under the normal operating conditions which is a unique property amongst emission sources. This understanding of the observed emission signals is vital to the development of the technique.

CHAPTER THREE

EXPERIMENTAL

3.1 INSTRUMENTATION

3.1.1 Atomic Absorption

The instrument used in this thesis was a Perkin Elmer model 306 spectrometer with a HGA74 heated graphite atomiser. The spectrometer is a double beam design with one of the beams acting as a reference and the other passing through the atom cell. This double beam system has advantages over a single beam system in that a warm up period is not required for the hollow cathode lamp and fluctuations in the lamp intensity do not have a critical effect during analysis.

The monochromator with this spectrometer employs a dispersion grating system of Czerny-Turner design, with a UV dispersion of 0.65nm per mm and a visible dispersion of 1.30nm per mm. The focal length is 400mm and the grating is ruled to 2800 lines per mm for the UV and 1440 lines per mm for the visible. The grating is blazed at 210nm for the UV and 600nm for the visible and the spectrometer is capable of scanning wavelengths between 180 and 900nm.

All atomic absorption measurements were made using the HGA74 furnace which uses electrothermal energy to provide an atom cloud instead of a conventional flame system. The atomiser and flame units are interchangable and both occupy the same position in this system. Controls on the furnace module allow the furnace to be moved vertically, horizontally and rotationally to ensure that the light from the hollow cathode lamp is focussed directly through the centre of the graphite tube. The graphite tube is supported at each end by a graphite cone which is fixed into the metal casing of the furnace. These cones transmit electrical power to the tube which acts as a resistance and so is heated, the tube temperature varying from ambient to 2700°C depending on the amount of current passed. The control unit governs the supply of power to the tube with both the current and voltage being variable to a maximum of 440 amps and 8 volts respectively. The large transformer when used with the timing mechanisms allows the temperature, of the tube, to be maintained constant for varying lengths of time. The 4 timing mechanisms are normally used for the drying, ashing, atomising and cleaning stages of the analytical program. There is an additional facility which allows for a ramp heating stage between the second and third preset stages for analysis which may require a slow build up to the atomisation temperature.

To prevent the oxidation of the graphite furnace at high temperature an inert gas, in this case argon, is continually circulated around and through the graphite furnace escaping via the sample injection port. This gas also acts as a flushing agent removing any unwanted vapour or smoke from the tube. Cold water is also circulated around the metal casing to prevent excessive heating of the end cones and furnace body and also to cool the tube allowing for shorter time intervals between subsequent sample injections. Temperature and gas sensing devices automatically cut the power supply when either the water or gas is not flowing, thereby preventing damage. During the atomisation stage the internal gas flow can be reduced from 350ml per minute to 50ml per minute by the use of miniflow and may be stopped altogether by using gas stop. Both these restrictions last for the first 8 seconds of the atomisation stage, however the external flow around the outside of the furnace is not affected by the use of these gas flow restrictions.

3.1.2 Atomic Emission

The instrument used for atomic emission measurements is not commercially available but is one which was assembled in this laboratory about three years ago[48,49]. The basic components of the instrument are readily available and are illustrated in Figure 3.1.1 which shows a schematic diagram of the system. Atomisation of the sample to produce the emission spectra was achieved using a HGA72 furnace. The graphite tube in this furnace is considerably larger than the HGA74 type, having a length of 53mm extermal diameter 10.5mm and and internal diameter of 8.65mm compared with 28.1mm, 8mm and 6.2mm of the HGA74 tube. The gas flow pattern within the tube is also different as the inert gas is introduced through the dosing hole and also through two holes in each end of the tube. Other aspects of the furnace are similar to the HGA74 and the control unit is the same for both furnaces.

A long focus lens(f = 130mm) was used to focus the light from the centre of the furnace on to the entrance slit while preventing any direct tube wall emission from entering the monochromator. The Spectrametrics SMI echelle monochromator employs a high resolution grating which rejects much of the background radiation from the tube thereby allowing for a better processing of the analytical signal. A wavelength modulation chopper is located at the exit slit from the monochromator driven by an external power supply which also provides a reference signal. The photomultiplier signals are amplified by a pre-amplifier and then processed by

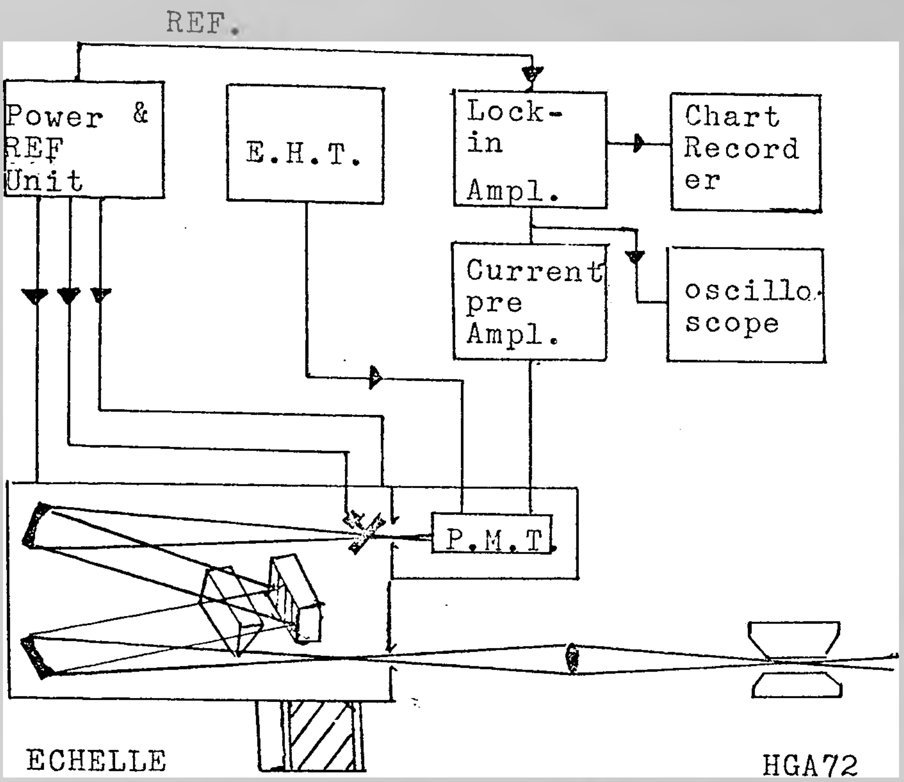

Figure 3.1.1

Schematic diagram of the
Atomic Emission System

an Ortec Brookdeal lock-in amplifier. This signal was displayed on a Servoscribe potentiometric recorder.

The unusual feature of this instrument is the wavelength modulation system employed within the spectrometer. The rotating chopper located at the exit slit consists of four separate quadrants each made of quartz and mounted at an incident angle of about 45°. Two of the sectors in opposite quadrants have the same thickness, while the other two have different thicknesses, one larger and the other equally smaller than the two identical quadrants. With the refraction of light passing through the quartz sectors depending on the thickness of the quartz it has been arranged that the wavelength of the light leaving the exit slit of the monochromator, alternates between the analyte atomic wavelength and preselected wavelengths, at an equal but opposite displacement on either side of the analyte line. The lock-in amplifier measures and subtracts the two background signals from the analyte signal thereby achieving efficient background correction. This square wave wavelength modulation system improves the signal to noise ratio by a factor of 1.8 compared to a sine-wave system.

3.1.3 Signal Recorder

The signals obtained by atomic absorption were recorded using a Perkin Elmer 56 chart recorder in which 10mv full scale deflection is equivalent to 1 absorbance unit. Direct readings from the visual display were recorded along with the chart trace with the use of the peak height facility. The recorder also initiates a servo system so that only the signal during the atomisation stage was recorded.

Atomic emission signals were recorded using a Servoscribe RE 541.20 strip chart recorder. This also incorporates a servo system allowing only the signal during the atomisation stage to be measured.

3.1.4 Temperature Measurements

The tube wall and platform temperatures of both furnaces were measured with an Ircon Series 1100 optical pyrometer. The pyrometer was focused on the inside of the tube through the sample injection hole. Temperatures during the atomisation period were recorded on a Servoscribe RE 541.20 chart recorder at a speed of 1cm per second.

3.1.5 Platforms

The platforms used in these studies were made from standard

HGA72 and HGA74 tubes. The dimensions of the HGA72 platforms were approximately 11 x 8mm and the HGA74 7 x 5mm, the thickness of both being the same as that of the tube wall. Only the edges of the platforms were in contact with the tube wall. The platforms used in conjunction with the tantalum coated tubes were also coated with tantalum using Zatka's procedure.

3.1.6 Sample Introduction

Injection of liquid samples was accomplished by a micro pipetting sampler manufactured by Oxford Laboratories. The sampler uses precision moulded, non wettable plastic tips. This enables the operator to eliminate pipette cleaning, the danger of contamination and error due to variation of technique. The reproducibility of the pipettes used is approximately 2%. The pipette tips used were also manufactured by Oxford.

3.1.7 Light Source

The indium lamp used was a Perkin Elmer "Intensitron" Hollow Cathode lamp. The lamp dimensions are 5cm in diameter and 18.5cm in length. The lamp was operated at a current of 20mA with the slit width of the instrument set at 0.7nm.

3.2.1 Sample Collection and Preparation

The samples used for the analyses reported in this thesis were collected from various well known mining localities in Scotland and the North of England by the author and from Silvermines in Eire by Ian Samson of the Applied Geology Department, University of Strathclyde. With the exception of this locality the other localities are not now productive sites. Because of the danger of entering abandoned mine workings samples were taken from the spoil leaps associated with the various mines. This factor is not crucial as only the feasibility of determining indium in the ores was being investigated and no geological significance is placed upon the results. The sample localities are given in Table 3.2.1.

The samples used were those which contained large concentrations of the pure ore which could be easily removed from the gangue material by mechanical means. The ore was then crushed in a stainless steel swing mill until all the sample could be passed through a 100 mesh seive. This required about 2½ minutes of crushing. The sample was dried at 110°C for 2 hours to remove any moisture and stored in self-sealing plastic bags until required for analysis.

TABLE 3.2.1

Sample Localities of Galena and Sphalerite

Ore	Sample Number	Locality	Map Reference
Sphalerite	1,	Leadhills-Wanlockhead	Sheet 68 893 141
	2,3,4,5,	"	Sheet 68 887 139
	6,	"	Sheet 68 884 139
	7,8,9,	"	Sheet 68 864 134
	10,11,12,13,14,	Tyndrum	Sheet 50 317 305
	15,	Silvermines	Not known
Galena	1,2,3,4,	Leadhills-Wanlockhead	Sheet 68 864 134
	5,6,7,	Pikestone Brow	Sheet 84 995 294
	8,	Leadhills-Wanlockhead	Sheet 68 884 139
	9,	Cawood Hill	Sheet 87 702 429
	10,11	Tyndrum	Sheet 50 317 305
	12,13,14,	Ley Seat	Sheet 84 828 200

3.2.2 Sample Dissolution Procedure

Galena

1g of the crushed ore was dissolved with 10ml of 50% nitric acid in a 250ml pyrex beaker covered with a watch-glass. The sample was gently heated to just below boiling to ensure complete dissolution. The solution was then cooled, 5ml of concentrated sulphuric acid added, mixed and the mixture allowed to stand for 10 minutes, The entire contents of the beaker were transferred, washing with distilled water, to a filter funnel and filtered through a pulp pad into a 100ml graduated flask which was retained for analysis. All additions of acid were made by pipette.

As the large concentrations of lead were shown to cause interference by condensation on the quartz windows of the HGA74 furnace, the above procedure was chosen so that most of the lead would be precipitated. However, the indium remains in solution and is not precipitated along with the lead.

3.2.3 Sphalerite

0.5g of the crushed ore was dissolved with 20ml of 50% v/v nitric acid in a 250ml pyrex beaker covered with a watchglass. The sample was heated gently and allowed to simmer for 30 minutes until the globules of sulphur turned bright yellow. The solution was allowed to cool and filtered through a Whatman No 541 filter paper and diluted to 100ml with distilled water in a volumetric flask which was then used for the analysis. Addition of the solvent acid was made by pipette.

Initially the sulphur was retained to ensure that no indium was contained within it. This was checked by direct introduction of the sulphur to the furnace and subsequent atomisation and by burning of the sulphur at low temperature, extracting with a drop of nitric acid and subsequent atomisation in the furnace. No indium was detected in either case.

3.3 TANTALUM COATING OF GRAPHITE TUBES

The method of tantalum treatment used was virtually identical to that described by Zatka[42] with one exception. The tubes were first immersed in the tantalum solution contained in a plastic dish. In Zatka's procedure the dish was transferred to a desiccator and the pressure reduced using a water pump, here the dish was placed in the vacuum chamber of an argon-arc remelter and the pressure reduced to 10 torr for approximately 30 seconds. The atmospheric pressure was restored, the tubes removed from the solution, allowed to dry in the air for approximately 30 minutes and then at 110°C for approximately 1 hour. The tube was then fitted into the furnace, which contained new graphite cones, and over a period of about 30 seconds was heated to 1000°C and then raised quickly to 2500°C for 5 seconds. During this heating both the water and inert gas remained flowing. The soaking procedure was repeated with the reduced pressure being restricted to approximately 10 seconds duration. The drying and heating in the furnace were carried out identically with the initial treatment.

After the initial treatment and pyrolysis the weight of the tube had increased by approximately 0.7% and after the second soaking and pyrolysis the weight had increased by a total of approximately 1.3%. This increase due to deposition of tantalum amounted to approximately 0.0127g (average of 4 tubes) of tantalum.

3.4 REAGENTS

3.4.1 Distilled Water

The purity of the water for use in this work had to be that which contained low levels of any trace elements present. For this purpose an all glass still with a silica sheathed heating element was used. The still is manufactured by Quickfit Ltd. and supplies water at a rate of approximately 4 litres per hour, the water being stored in all plastic containers which had previously been washed with 20%v/v nitric acid and then with distilled water before use.

3.4.2 Tantalum Soaking Solution

3g of Koch Light high purity tantalum metal, 99.999%, was weighed into a 100ml PTFE beaker and 10ml of 50% v/v hydrofluoric acid, 3g of oxalic acid dihydrate, 0.5ml of 30% hydrogen peroxide added. The beaker was slowly heated to aid dissolution with more hydrogen peroxide being added when the reaction became too slow. When dissolution was complete a further 4g of oxalic acid was added along with 30ml of distilled water and allowed to dissolve. The solution was diluted to 50ml with distilled water and stored in a plastic bottle.

3.4.3 Stock Solutions

The stock solutions for the analyte element and the interference studies were prepared from the purest metals or compounds available and these are shown in

Table 3.4.1. The acids used were of 'Analar' grade with the specifications shown in Table 3.4.1.

TABLE 3.4.1

Stock Metal Solutions

Element	Form	% Purity	µg/ml	Acid Concentration
Copper*	Powder	99.9	1,000	1% HNO_3
Manganese*	Flake	99.995	1,000	1% HNO_3
Iron*	Powder	99.995	1,000	2% HNO_3
Zinc*	Wire	99.999	6,000	1% HNO_3
Lead	Powder(PbO)	99.8	10,000	1% HNO_3
Indium**	Powder	99.999	1,000	0.5% HNO_3

* Interference Studies

** Analyte Element

ACID SPECIFICATIONS

Acid	Specific Gravity	% Assay
Sulphuric	1.84	97 - 100
Nitric	1.42	69 - 71
Hydrochloric	1.18	31 - 32
Perchloric	1.70	71 - 73

CHAPTER FOUR

RESULTS AND DISCUSSION

4.1 INSTRUMENTAL PARAMETERS

4.1.1 Optimisation of Working Conditions

Table 4.1.1 shows the furnace operating conditions for the different types of furnace tube used for atomic absorption and atomic emission measurements. To ensure optimum atomisation of the sample each of the stages must be optimised in turn for the element in question. The drying stage was used to evaporate the solvent and a temperature of 100°C was found to be suitable. With the difference in temperature between the tube and platform the tube temperature was required to be raised above this value to ensure the platform reaches 100°C. The drying time, however, is governed by the size of the sample aliquot with 20µl or less requiring about 30 seconds and 50µl requiring about 45 seconds. Again because of the temperature lag with the platform an additional 10 seconds was added. In all cases the drying stage was monitored visually to ensure that drying was complete and that no spluttering of the sample within the tube occurred.

The temperature of the ashing stage is dependent on the temperature at which the element is volatilised. The

TABLE 4.1.1

Optimum Conditions for Various Atomisation Sources

	Drying		Ashing		Atomisation		Cleaning	
Atomiser	Digits	Secs	Digits	Secs	Digits	Secs	Digits	Secs
HGA74**								
Normal Tube	65	30	190	30	900	10	999	5
Pyrolytically Coated Tube	60	30	175	30	900	10	999	5
Tantalum Coated Tube	55	30	100	30	900	10	999	5
HGA74*								
Normal Tube/ Platform	70	40	120	30	900	10	999	5
Tantalum Coated Tube/ Tantalum Platform	60	40	110	30	870	10	999	5
HGA72***								
Normal Tube	38	45	110	30	930	8	999	5
Tantalum Coated Tube	40	45	100	30	930	8	999	5
Normal Tube/ Platform	68	55	105	30	930	8	999	5
Tantalum Coated Tube/ Tantalum Platform	68	55	110	30	930	8	999	5

* 10µl sample A.A.S. ** 20µl sample A.A.S.

*** 50µl sample A.E.S.

optimum temperature was found by conducting a series of experiments at varying temperatures to find at what temperature, losses during the ashing stage became significant. The use of the ashing stage was essential in that it removed the major part of the acid matrix, nitric and sulphuric acids, which would have produced smoke giving spurious results during atomisation. This stage also aids in converting the element to a form suitable for atomisation. The standard time of 30 seconds was found to be adequate for all the sample aliquots in that the major portion of the smoke from the solvent acids was removed during this period.

Similar experiments were carried out to determine the most efficient temperature for atomisation of the sample. The preset temperature is not necessarily the temperature at which atomisation takes place. The appearance of the atomic absorption signal takes place when the tube temperature is at approximately 1200°C and the atomic emission signal at approximately 1350°C.

The values given in Table 4.1.1 for the preset temperatures are arbitrary values, with the values for the two instrument systems being unrelated.

4.1.2 Furnace Temperature Profiles

The increase of the temperature of the two furnaces was recorded from 1800°C to the maximum value achieved over a 10 second atomisation period. The temperature profiles obtained are shown in Figs 4.1.1 and 4.1.2 and illustrate the heating rates for the two furnaces. These results were obtained by focusing the Ircon 1100 optical pyrometer on the heated tube through the injection hole. Profiles were obtained for normal and tantalum carbide coated tubes as well as for platforms made of the respective materials.

For both types of tube and platform the rate of heating was found to be identical. However the final temperature achieved by the tantalum coated tube and platform was less by about 30-50°C than the normal tube and platform. With the HGA72 furnace the time required for each type of tube to reach similar temperatures was the same during the initial stages but with the HGA74 a longer time was required by the tantalum coated tube to reach the temperature achieved by the normal tube. The effect of the platform can be clearly seen with the shifting of the temperature of the platform relative to the tube to longer times. The difference in the tube and platform temperatures at the same time during atomisation was found to be of the order of 300°C.

FIG 4.1.1

Temperature-Time Profile of HGA72 with Various Atomisation Sources

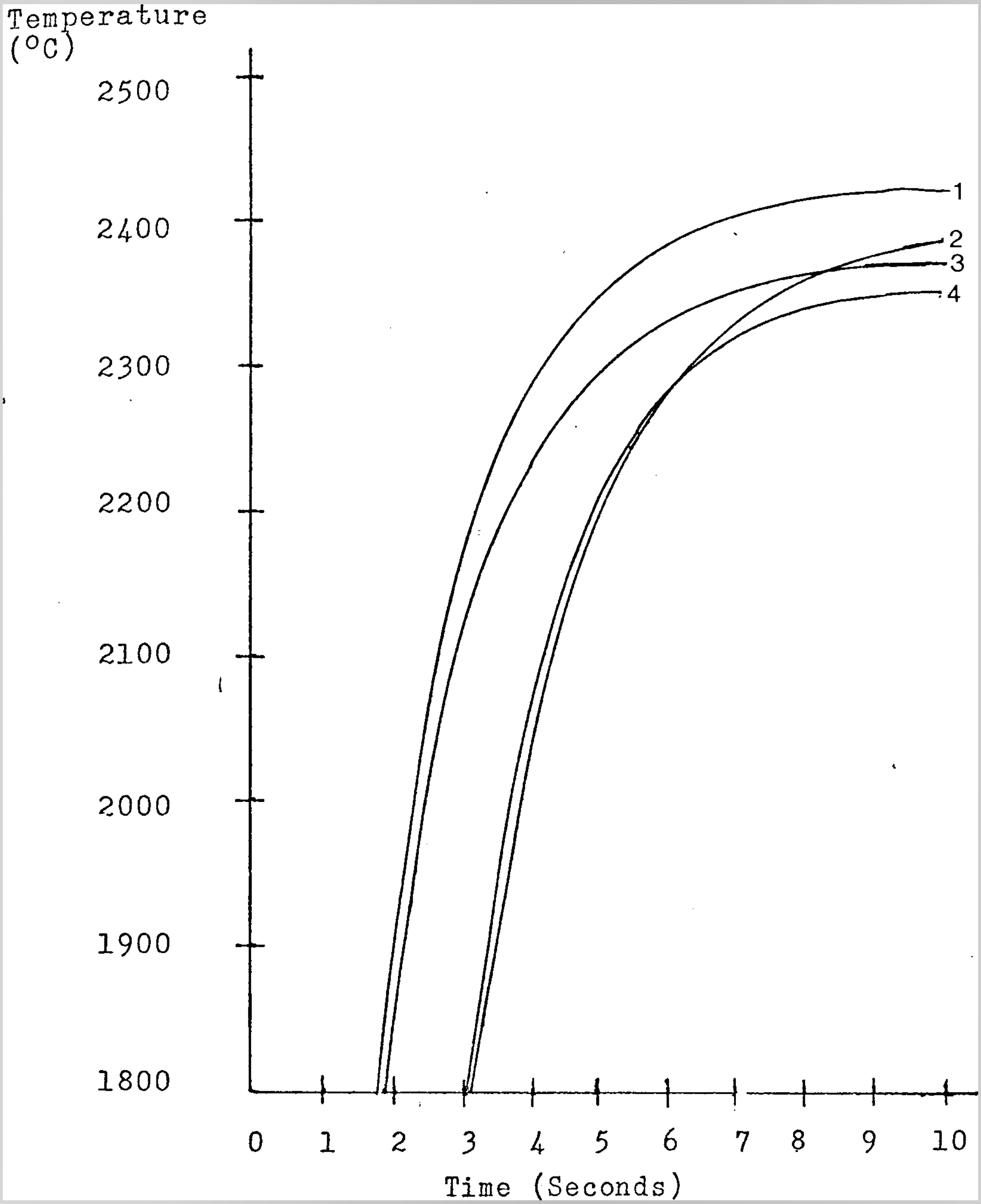

1. Normal Tube
2 Normal Tube/Platform
3 Ta Coated Tube
4 Ta Coated Tube/
Ta Coated Platform

FIG 4.1.2

Temperature-Time Profile of HGA74 with Various Atomisation Sources

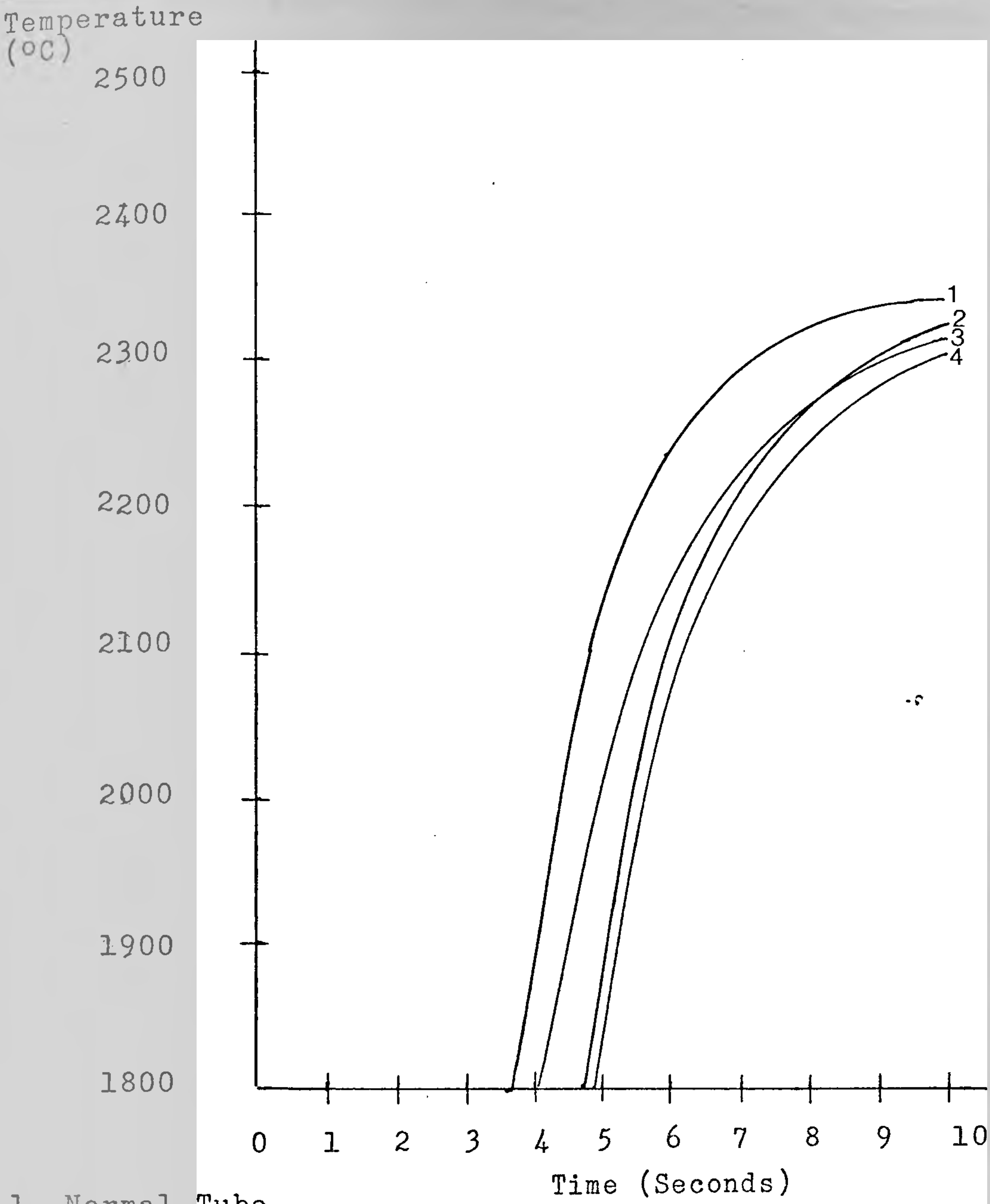

1 Normal Tube
2 Normal Tube/Platform
3 Ta Coated Tube
4 Ta Coated Tube/
Ta Coated Platform

4.1.3 Detection Limits, Precision and Sensitivity

The detection limits were determined for both the atomic absorption and atomic emission instruments and these are given in Table 4.1.2. With the HGA74 furnace the detection limits were determined for all the atomisation surfaces using the three different gas flow modes with the exception of the pyrolytically coated tubes which yielded double peaks when operated with gas stop. Only the detection limits with gas stop were determined using the HGA72 furnace as analysis of the samples by atomic absorption had been carried out and the levels of indium could not be detected with the furnace gas flowing during atomisation.

Atomic absorption detection limits were obtained by measuring the absorbance of two solutions one of which was approximately the same as the anticipated value the other solution containing approximately twice the concentration of the first. A sequence of measurements of the blank, first solution, blank and second solution was carried out until ten absorbance measurements had been recorded for each solution. Corrections for the blank were made and the mean and standard deviation for the two solutions calculated. The detection limit was defined as twice the standard deviation times the concentration divided by the mean absorbance, with the accepted detection limit being the average for the two solutions.

The atomic emission detection limit was defined as the concentration of indium equivalent to twice the standard deviation of the noise. The amplification of the instrument was increased until the noise could be easily measured. The slope of the calibration graph was determined near the detection limit by measuring three solutions ten times each with the noise being determined between each analyte solution.

From the results obtained it seems that the tantalum coating procedure carried out on the tubes improves the detection limit for atomic absorption but no significant improvement was found to occur for atomic emission. This improvement also holds for platforms coated with tantalum. The use of mini gas flow does not appear to improve the detection limit for indium as it does for some other elements. This is probably due to the fact that indium is easily volatilised and any gas flow through the furnace aids the expanding hot gas in removing the indium from the furnace. The use of platform atomisation also aids in lowering the detection limit by a factor of approximately four for atomic absorption and by about ten for atomic emission. The tubes and platforms used in emission measurements were not coated with pyrolytic graphite as is normal since a direct comparison of the effect of the tantalum coating was being investigated. The detection limits are given in Table 4.1.2.

The precision of the measurement of the aqueous standards at various concentrations are given in Table 4.1.3. The R.S.D. values were computed in the normal manner for ten analytical determinations of each standard under gas stop conditions.

The sensitivities obtained for the various atomisation surfaces are given in Table 4.1.4. These were calculated to be the concentration of the element which absorbs one percent of the incident resonance radiation of the element, that being an absorbance of 0.0044. All the sensitivities were calculated from calibration graphs from which the rate of change of absorbance with concentration was obtained.

In the preceeding measurements, 20µl aliquots were used when the tube alone was the atomisation source, but with the platform a 20µl sample was found to be difficult to place on the platform without touching the tube wall. In this case the sample aliquot was reduced to 10µl which could be accurately positioned.

4.2 INTERFERENCE STUDIES

4.2.1 Effect of Various Acids

Before a suitable dissolution procedure for the samples

TABLE 4.1.2

Detection Limits for Aqueous Standards

Atomiser	Normal Flow µg/ml	Mini Flow µg/ml	Gas Stop µg/ml
HGA74**			
Normal Tube	0.084	0.083	0.0032
Pyrolytically Coated Tube	0.053	0.040	-
Tantalum Coated Tube	0.013	0.014	0.0016
HGA74*			
Normal Tube/Platform	0.019	0.020	0.0020
Tantalum Coated Tube/ Tantalum Platform	0.012	0.0098	0.00078
HGA72***			
Normal Tube	-	-	0.0011
Tantalum Coated Tube	-	-	0.0011
Normal Tube/Platform	-	-	0.000085
Tantalum Coated Tube/ Tantalum Coated Platform	-	-	0.00011

*	10µl sample A.A.S.	303.94nm
**	20µl sample A.A.S.	303.94nm
***	50µl sample A.E.S.	451.1nm

TABLE 4.1.3

Reproducibility for the Measurement of Standards at Various Concentrations Under Gas Stop Conditions

Atomiser	µg/ml	R.S.D.%	µg/ml	R.S.D.%	µg/ml	R.S.D.%
HGA74**						
Normal Tube	0.005	24.9	0.01	10.8	0.10	1.6
Tantalum Coated Tube	0.005	22.1	0.01	9.3	0.10	1.5
HGA74*						
Normal Tube/ Platform	0.005	29.6	0.01	8.8	0.05	2.4
Tantalum Coated Tube/ Tantalum Platform	0.005	20.4	0.01	11.9	0.05	3.2
HGA72***						
Normal Tube	0.01	11.7	0.03	5.6	0.05	2.0
Tantalum Coated Tube	0.01	5.7	0.03	2.7	0.05	1.8
Normal Tube/ Platform	0.001	7.6	0.003	3.4	0.005	1.5
Tantalum Coated Tube/ Tantalum Platform	0.001	10.6	0.003	5.8	0.005	3.7

*	10µl sample A.A.S.
**	20µl Sample A.A.S.
***	50µl sample A.E.S.

In some cases the concentrations used were close to the detection limit and the R.S.D. values do not reflect the performance of the atomiser under optimum conditions.

TABLE 4.1.4

Sensitivity of Various Atomisation Sources

Atomiser	Normal Flow	Mini Flow	Gas Stop
	μg ml^{-1}		
Normal Tube**	0.062	0.063	0.0034
Pyrolytically** Coated Tube	0.055	0.055	-
Ta Coated Tube**	0.0099	0.0101	0.0021
Normal Tube/* Platform	0.018	0.018	0.0022
Ta Coated* Tube/Platform	0.014	0.014	0.0018

* 10µl sample

** 20µl sample

could be formulated the effect of the four possible solvent acids on the indium signal had to be determined. The four acids considered were nitric, sulphuric, perchloric and hydrochloric. The effects which were observed for each acid using atomic absorption are presented in Tables 4.2.1 - 4 and represent the percentage change in the signal obtained for 0.1µg/ml indium with the furnace operated in the gas stop mode. The 0.1µg/ml indium gave an adequate signal of about 0.2 absorbance units and the effect of the varying acid concentrations, 0.1, 0.3, 0.5, 1.0, 3.0, 5.0 and 10.0%, could be observed with reasonable accuracy. Blank solutions of 10.0% acid concentration, without any analyte element added were analysed to check for any possible indium in the acids. This was thought unlikely because of the rarity of the element and the blanks showed no trace of any indium. 20µl and 10µl aliquots were used for the tubes and platforms respectively. The percentage interference caused by acid was calculated from the change of the signal obtained from a standard aqueous solution at the same analyte concentration, i.e.

$$\%\ \text{Interference} = \frac{(\text{Signal for Acid Standard} - \text{Signal for Aqueous Standard}) \times 100\%}{\text{Signal for Aqueous Standard}}$$

The results given were obtained from an average of three injections for each of the acid solutions.

Nitric acid gives an enhancement in the indium signal, which for the normal graphite tube increases with concentration to a maximum and then remains relatively constant. The tantalum coated tube and the platforms do not exhibit similar characteristics. These initially show an enhancement of the signal but with increasing acid concentration this lessens and at 10% acid no real enhancement occurs.

With sulphuric acid both the normal tube and platform exhibit an enhancement which increases with concentration until a maximum is reached in both cases at about 1% acid. The tantalum coated tube and platform both show a similar trend with an initial enhancement followed by a reduction but in contrast to nitric acid the effect does not decrease to zero.

Both perchloric and hydrochloric acids cause a large decrease in the observed signal of over 90% with perchloric acid and about 70% with hydrochloric acid both at the 10% concentration level. The depression caused by hydrochloric acid is most probably due to losses caused by volatilisation of molecular chloride species. Perchloric acid or its decomposition products on the other hand apparently interact with the graphite of the tube to form thermally stable compounds which are released during the atomisation stage. These probably then form molecular species with the analyte atoms thus severely suppressing the peak height absorbance.

TABLE 4.2.1

The Effect of Nitric Acid on the Indium Signal

	Atomisation Source			
% v/v Acid	Normal Tube	Normal Tube/ Platform	Ta Tube	Ta Tube/ Ta Platform
0.1	+ 39	+41	+20	+37
0.3	+ 55	+31	+14	+22
0.5	+ 74	+27	+ 7	+16
1.0	+ 82	+12	+ 2	+13
3.0	+122	+10	Nil	+ 9
5.0	+132	+ 6	- 1	+ 6
10.0	+139	+ 1	- 2	+ 4

+ ve Enhancement

- ve Depression

TABLE 4.2.2

The Effect of Sulphuric Acid on the Indium Signal

	Atomisation Source			
% v/v Acid	Normal Tube	Normal Tube/ Platform	Ta Tube	Ta Tube/ Ta Platform
0.1	+48	+ 58	+47	+41
0.3	+57	+ 81	+37	+30
0.5	+59	+ 94	+35	+26
1.0	+72	+104	+32	+26
3.0	+74	+104	+28	+24
5.0	+76	+105	+26	+24
10.0	+78	+106	+23	+19

+ve Enhancement

-ve Depression

TABLE 4.2.3

The Effect of Perchloric Acid on the Indium Signal

	Atomisation Source			
% v/v Acid	Normal Tube	Normal Tube/ Platform	Ta Tube	Ta Tube/ Ta Platform
0.1	-23	-64	-64	-56
0.3	-40	-74	-66	-64
0.5	-51	-83	-68	-71
1.0	-57	-85	-69	-76
3.0	-69	-89	-80	-86
5.0	-77	-92	-90	-93
10.0	-83	-97	-92	-93

+ve Enhancement

-ve Depression

TABLE 4.2.4

The Effect of Hydrochloric Acid on the Indium Signal

% v/v Acid	Atomisation Source Normal Tube	Normal Tube/ Platform	Ta Tube	Ta Tube/ Ta Platform
0.1	-31	-26	-59	-35
0.3	-33	-35	-61	-38
0.5	-40	-42	-63	-42
1.0	-48	-46	-48	-48
3.0	-55	-53	-73	-52
5.0	-59	-60	-78	-56
10.0	-66	-70	-80	-66

+ve Enhancement

-ve Depression

As stated earlier the individual acids did not give any absorbance, however the blank combination of 5% nitric and sulphuric acids, as used in the dissolution of galena, did show a significant absorbance. This has been proposed[50] as due to the interaction of the two acids with the graphite forming graphite hydrogensulphate of the type $C^{+}_{m}HSO^{-}_{4} \cdot 4HSO_{4}$. These type of compounds are not completely decomposed during the ashing stage but produce volatile species during atomisation. The absorption bands of these molecules overlap the absorption line of the analyte atom causing the higher blank absorbances. The likely cause of these volatile compounds is a series of reactions involving C, SO_2, SO, S_2 and COS.

The deterioration of the tubes was most noticable with the normal tube which soon became very fragile, but the tantalum coated tube on the other hand resisted the acid attack much better although it also showed signs of failure after approximately 250 injections compared with about 60 for the normal tube.

4.2.2 Effect of Metal Ions

From various literature sources it was found that around thirty elements could be found in minor concentrations in galena and sphalerite. Many factors influence the distribution of the trace elements including whether the ore is syngenetic, epigenetic, sediment hosted, associated with acid magmatism etc. One of the major factors is the temperature of deposition of the ore which can be used to estimate the elements which are likely to be present in significant quantities. In general the localities from which the samples were taken tended to be low temperature deposits. Related to the temperature, sphalerite contains appreciable quantities of iron which is present in the ore as iron sulphide and it was decided to analyse for this. Analysis was by titration with potassium dichromate after dissolution of the sample in hydrochloric acid. The results are presented below.

Sample No	1	2	3	4	5	6	7	8	9	10	11	12	13	14	15
% Fe	2.8	2.5	2.5	2.8	2.7	2.2	3.2	3.4	3.5	0.7	0.8	0.8	0.7	0.6	0.5

It was decided that with these specific localities only five metals required to be examined as to their effect on the indium signal. These metals were lead, zinc, iron, copper and manganese. Tables 4.2.5-9 show the effects each of these elements has on the indium atomic absorption signal. The maximum concentrations used reflect the highest values of these elements thought likely to be present after consideration of the concentrations found in similar deposits. It is probable that the samples used do not contain the maximum concentrations used. As the standard solutions all contain nitric acid a further 5% nitric acid was added to each metal solution used in order to match the acid matrix.

Both acid and metal interference studies were carried out using the HGA74 furnace. Each of the different atomisation surfaces was used and the furnace was operated in the gas stop mode. The optimum conditions given in Table 4.1.1 were used with each of the different surfaces. 20µl samples were used except with platform atomisation when 10µl samples were used. Background correction was not used during the interference studies.

The large concentrations of lead appear to have a considerable effect on the atomic absorption signal. However the enhancement is almost entirely due to the lead vapour causing a decrease in the amount of radiation transmitted through the furnace. It is probable that this vapour is condensing on the quartz windows during atomisation when the gas in the furnace is not flowing. Indeed the clouding is noticable after one atomisation with the 10,000µg/ml lead solution. Further support is gained for this as no significant enhancement is observed when atomisation is carried out with the end windows removed or when the furnace is operated under gas flow conditions. Table 4.2.10 shows that lead,zinc and iron give no significant enhancement of the indium signal when

TABLE 4.2.5

The Effect of Copper on the Indium Signal

	Atomisation Source			
µg/ml	Normal Tube	Normal Tube/ Platform	Ta Tube	Ta Tube/ Ta Platform
10	- 9	+ 1	+ 2	nil
30	-11	+ 4	+ 4	+ 4
50	-10	+ 9	+ 8	+ 6
70	-12	+14	+ 9	+ 9
100	-13	+17	+11	+13

+ve Enhancement

-ve Depression

TABLE 4.2.6

The Effect of Manganese on the Indium Signal

	Atomisation Source			
µg/ml	Normal Tube	Normal Tube/ Platform	Ta Tube	Ta Tube/ Ta Platform
1	- 6	+1	nil	+2
10	- 8	+4	+2	+4
30	-10	+6	+4	+5
50	-13	+7	+7	+9

+ve Enhancement

-ve Depression

TABLE 4.2.7

The Effect of Iron on the Indium Signal

	Atomisation Source			
μg/ml	Normal Tube	Normal Tube/ Platform	Ta Tube	Ta Tube/ Ta Platform
50	- 2	+ 6	+3	+ 4
200	- 5	+ 7	+3	+ 4
400	- 8	+ 9	+5	+ 5
700	-12	+11	+7	+ 7
1,000	-14	+15	+8	+11

+ve Enhancement

-ve Depression

TABLE 4.2.8

The Effect of Zinc on the Indium Signal

	Atomisation Source			
µg/ml	Normal Tube	Normal Tube/ Platform	Ta Tube	Ta Tube/ Ta Platform
500	- 6	+ 4	+2	+2
2,000	-10	+ 8	+3	+4
4,000	-15	+10	+4	+6
6,000	-18	+14	+5	+7

+ve Enhancement

-ve Depression

TABLE 4.2.9

The Effect of Lead on the Indium Signal

	Atomisation Source			
µg/ml	Normal Tube	Normal Tube/ Platform	Ta Tube	Ta Tube/ Ta Platform
50	+ 1	nil	+ 2	+ 3
100	+ 2	+ 3	+ 4	+ 5
500	+ 8	+ 9	+18	+ 7
1,000	+21	+19	+21	+18
3,000	+44	+40	+41	+39
6,000	+62	+59	+62	+60
10,000	+76	+72	+74	+70

+ve Enhancement

-ve Depression

TABLE 4.2.10

Effect of Lead, Zinc and Iron on the Indium Signal with Gas Flow Conditions in a Tantalum Coated Tube

Lead		Zinc		Iron	
µg/ml	Effect	µg/ml	Effect	µg/ml	Effect
50	-2	500	nil	50	+1
100	nil	2,000	-2	200	+3
500	-1	4,000	+3	400	nil
1,000	+3	6,000	+2	7,000	+2
3,000	+4			1,000	+6
6,000	+2				
10,000	+5				

+ve Enhancement

-ve Depression

atomisation is carried out with the gas flowing. Since to attain the required low levels of detection required for the analysis of galena, gas stop had to be used. Most of the lead was removed prior to the sample being atomised. The other metals produce a depression of the atomic absorption signal when atomised in the normal graphite tube but with the tantalum coated tube and with platform atomisation the signal is enhanced. Blank solutions of the highest metal concentration with the exception of lead did not produce any signal when atomised.

The results show that there is very little chemical interference by these elements on the indium signal when carried out in a 5% nitric acid matrix. The HGA74 does cause problems with the condensation of large quantities of some elements on the windows. This physical/spectral interference cannot occur in the HGA72 as the furnace is open ended. Time did not allow full investigation of interferences in CFAES but since the HGA72 was the atomiser used it was expected that there would be few. It was decided to proceed to the analysis of samples and to compare CFAAS results with CFAES as a check on the accuracy of the procedures.

4.3 ANALYSIS OF SAMPLES

The analysis of collected samples was carried out by both atomic absorption and atomic emission spectrometry. Except for some galena samples which contained too little indium to be determined by atomic absorption, satisfactory agreement between the results was obtained.

Atomic absorption analysis of both ores was carried out using tantalum coated tubes as the atomiser. These were chosen because of their good sensitivity and especially because of their higher resistance to attack by the acid matrix. Background correction was not used during the analysis. The atomic emission analysis of sphalerite was again carried out using tantalum coated tubes but in the analysis of galena a tantalum coated platform was used in conjunction with a similarily coated tube. Background correction was used in atomic emission analysis. Gas stop conditions were employed in both the HGA72 and HGA74 furnaces during analysis and the optimum conditions described in Table 4.11 were used.

Two methods were used in the determination, one involving a calibration graph using standards prepared in acid and the other by standard addition. The standards for the acid calibration graph were prepared in the same acid matrix as was used for the sample solutions. A solution blank was prepared for each set of samples being treated in the same way as the samples. Separate dissolution of samples for measurement by atomic absorption and atomic emission was used. The graphs in Figures 4.3.1 and 4.3.2 show typical standard addition and acid calibration graphs for galena and sphalerite, obtained by atomic absorption and atomic emission. Standard addition was carried out by the addition of three different aliquots of indium which with the original solution gave four points from which the graphs were constructed. These graphs were drawn manually and also computed using a linear regression technique. The acid calibration graph was also drawn manually and again by linear regression. The results obtained are given in Tables 4.3.1 to 4.3.4 and the indium values obtained show a good agreement between the methods of calculation. Table 4.3.5 compares the results of the two instrumental methods and Figs 4.3.3 and 4.3.4 show graphically the comparison using linear regression. The comparison for sphalerite is good but galena is less so mainly due to the lack of points.

Using the standard addition data the slopes were obtained (a) by drawing the graph and subsequent calculation and (b) by linear regression. The acid calibration slopes were also calculated in a similar manner from the obtained data. Tables 4.3.6 and 4.3.7 show the slopes for sphalerite and galena samples by both absorption and emission techniques. The mean value for the samples agrees closely with the acid calibration values in all cases enhancing the fact that there is probably no

FIG 4.3.1

Standard Addition and Acid Calibration Graphs by Atomic Absorption

(a) Galena

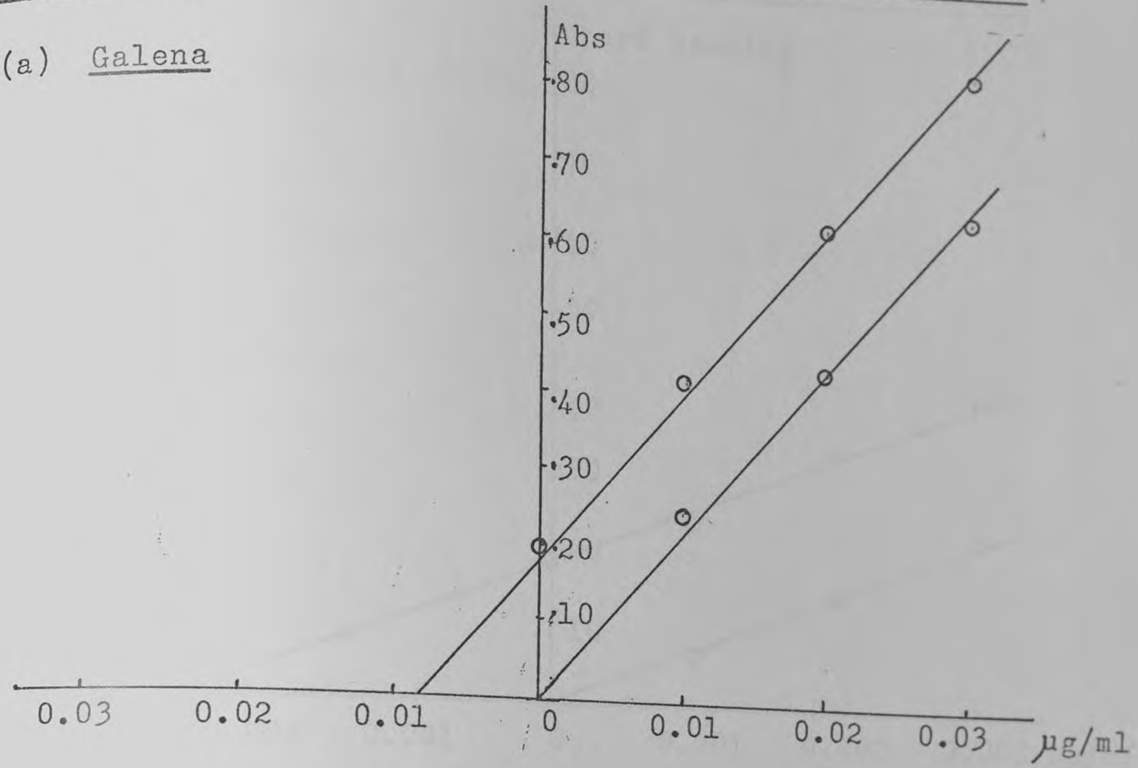

(b) Sphalerite

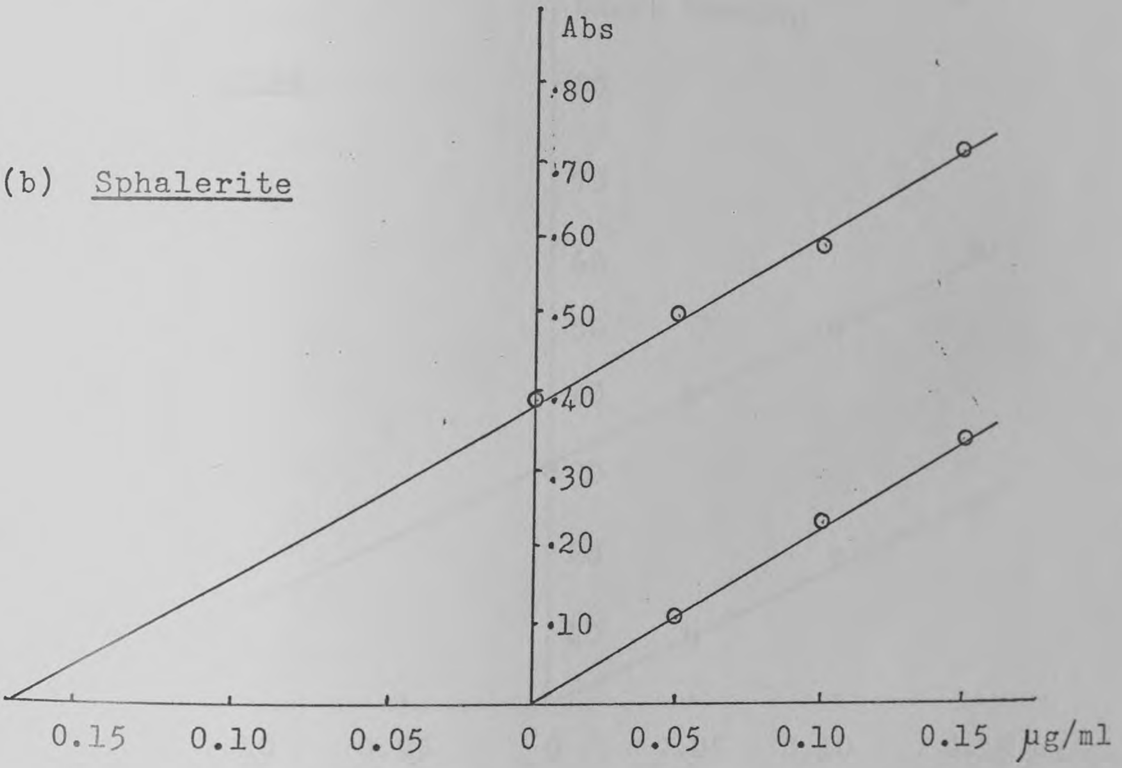

FIG 4.3.2

Standard Addition and Acid Calibration Graphs by Atomic Emission

(a) Galena

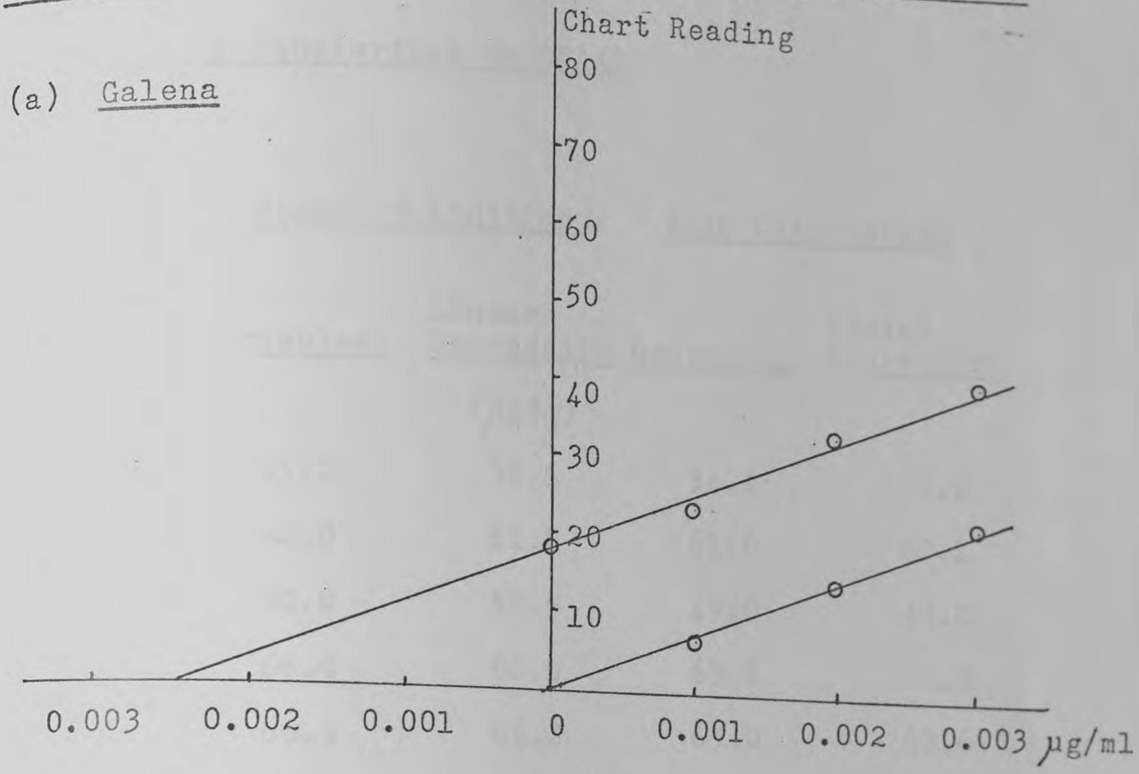

(b) Sphalerite

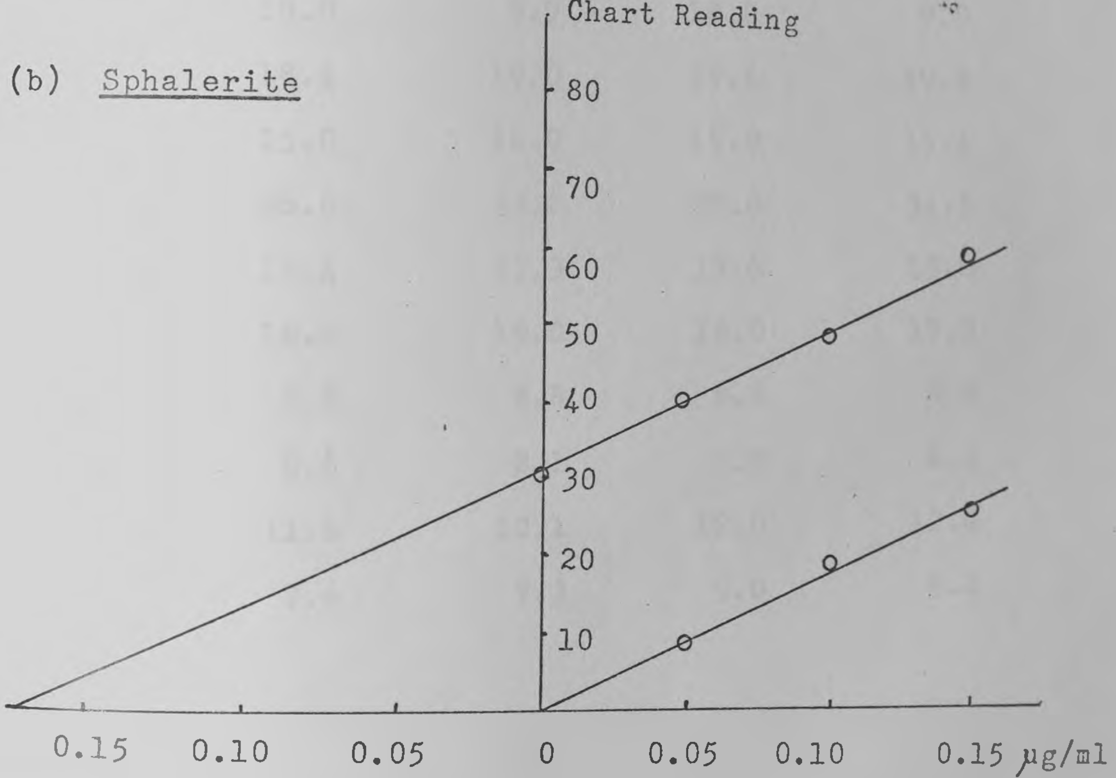

TABLE 4.3.1

Analysis of Sphalerites by CFAAS

	Standard Addition		Acid Calibration	
Sample No	Graphical	Linear Regression	Graphical	Linear Regression
		(μg/g)		
1	35.2	35.5	34.4	33.8
2	62.0	61.7	61.6	60.1
3	50.0	50.5	49.0	48.2
4	66.0	60.5	63.6	62.0
5	66.4	66.8	65.0	63.6
6	10.0	9.9	10.0	9.9
7	18.4	19.0	19.6	19.2
8	15.0	16.0	15.0	15.1
9	36.6	33.0	35.0	34.5
10	15.4	15.3	15.6	15.6
11	18.0	19.0	18.0	17.7
12	8.0	8.8	8.6	8.8
13	6.6	8.1	8.0	8.2
14	11.6	12.1	12.0	12.0
15	7.6	7.3	9.0	9.2

TABLE 4.3.2

Analysis of Sphalerites by CFAES

	Standard Addition		Acid Calibration	
Sample No	Graphical	Linear Regression	Graphical	Linear Regression
		(µg/g)		
1	33.0	34.0	34.0	34.3
2	59.6	60.9	62.0	62.1
3	48.0	48.7	49.0	49.0
4	62.0	62.8	61.0	61.0
5	65.0	66.6	64.0	64.3
6	10.4	10.8	10.4	10.4
7	18.0	19.1	19.4	19.6
8	14.4	14.7	15.4	15.3
9	33.6	33.6	34.0	34.0
10	15.6	15.5	16.0	15.8
11	18.4	18.9	21.0	19.6
12	11.0	10.8	10.0	9.8
13	6.4	7.6	8.0	8.2
14	11.0	11.6	12.0	12.0
15	7.6	8.5	7.0	7.7

TABLE 4.3.3

Analysis of Galenas by CFAAS

	Standard Addition		Acid Calibration	
Sample No	Graphical	Linear Regression	Graphical	Linear Regression
		(µg/g)		
1	0.18	0.20	0.10	0.10
2	< D.L.	< D.L.	< D.L.	< D.L.
3	< D.L.	< D.L.	< D.L.	< D.L.
4	0.55	0.57	0.55	0.48
5	< D.L.	< D.L.	< D.L.	< D.L.
6	< D.L.	< D.L.	< D.L.	< D.L.
7	< D.L.	< D.L.	< D.L.	< D.L.
8	0.85	0.83	0.87	0.83
9	0.23	0.15	0.20	0.24
10	0.33	0.37	0.35	0.23
11	< D.L.	< D.L.	< D.L.	< D.L.
12	< D.L.	< D.L.	< D.L.	< D.L.
13	< D.L.	< D.L.	< D.L.	< D.L.
14	< D.L.	< D.L.	< D.L.	< D.L.

TABLE 4.3.4

Analysis of Galenas By CFAES

	Standard Addition		Acid Calibration	
Sample No	Graphical	Linear Regression (µg/g)	Graphical	Linear Regression
1	0.24	0.24	0.25	0.25
2	0.10	0.10	0.11	0.10
3	0.08	0.09	0.09	0.09
4	0.48	0.50	0.50	0.49
5	0.06	0.07	0.07	0.06
6	0.03	0.05	0.05	0.04
7	0.08	0.10	0.10	0.09
8	0.77	0.79	0.80	0.80
9	0.21	0.23	0.23	0.21
10	0.35	0.35	0.34	0.34
11	0.07	0.08	0.08	0.07
12	0.06	0.06	0.07	0.06
13	0.03	0.04	0.03	0.03
14	0.04	0.03	0.04	0.04

TABLE 4.3.5

Comparison Between CFAAS and CFAES Sample Results

	Sphalerites			Galena	
Sample No	AAS (μg/g)	AES	Sample No	AAS (μg/g)	AES
1	34.7	33.8	1	0.15	0.24
2	61.4	61.2	2	< D.L.	0.10
3	49.4	48.7	3	< D.L.	0.09
4	63.0	61.7	4	0.54	0.49
5	65.5	65.0	5	< D.L.	0.06
6	10.0	10.5	6	< D.L.	0.04
7	19.1	19.0	7	< D.L.	0.09
8	15.3	15.0	8	0.85	0.79
9	34.8	33.8	9	0.21	0.22
10	15.5	15.7	10	0.32	0.35
11	18.2	19.5	11	< D.L.	0.07
12	8.6	10.4	12	< D.L.	0.06
13	7.7	7.6	13	< D.L.	0.03
14	11.9	11.7	14	< D.L.	0.04
15	8.3	7.7			

FIG 4.3.3

Comparison Between CFAAS and CFAES for Sphalerite Analysis

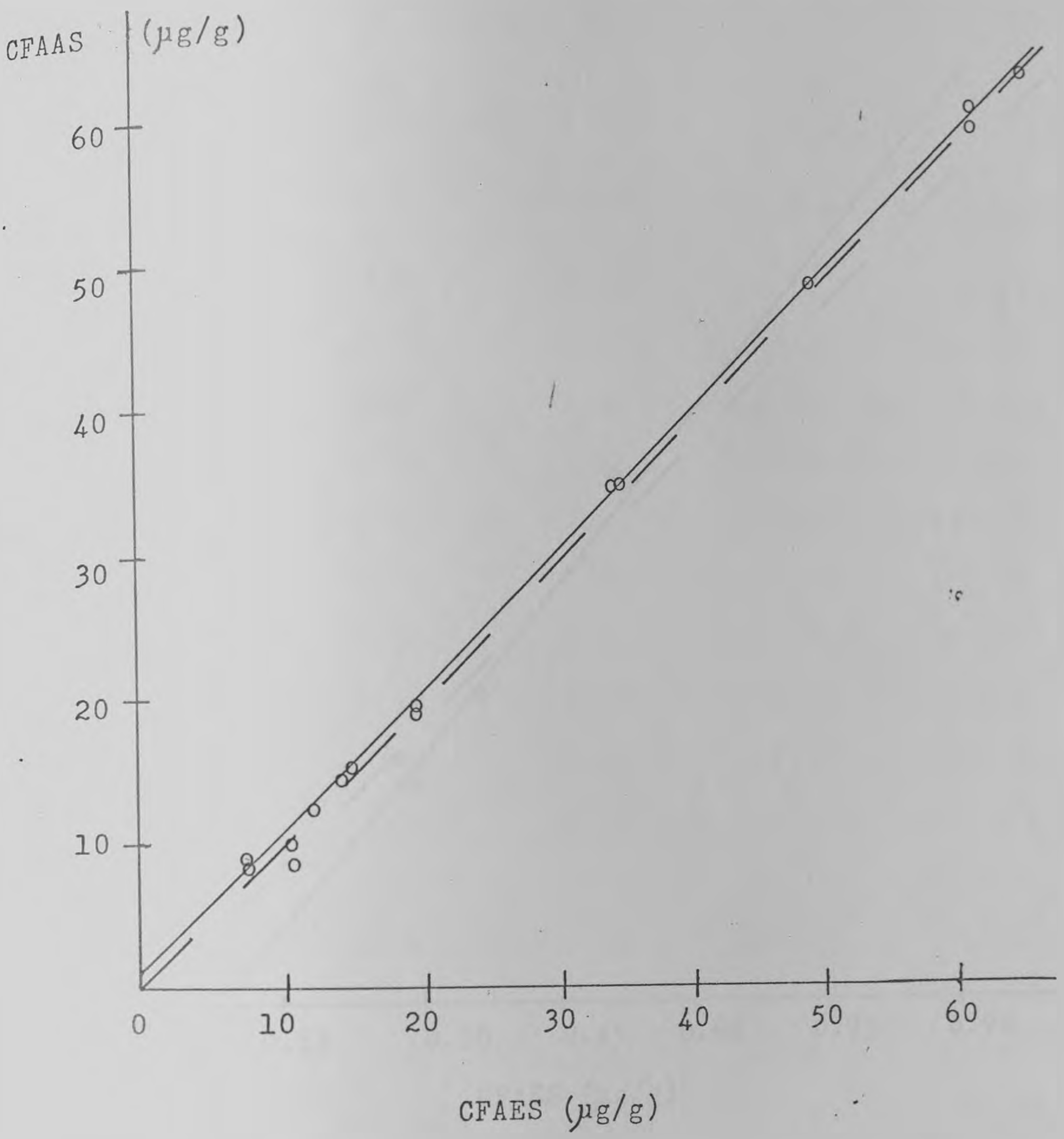

Slope	1.02
Correlation coefficient	0.9995
Intercept	0.023 µg/g

--- 45° line

____ Linear Regression graph

FIG 4.3.4

Comparison Between CFAAS and CFAES for Galena Analysis

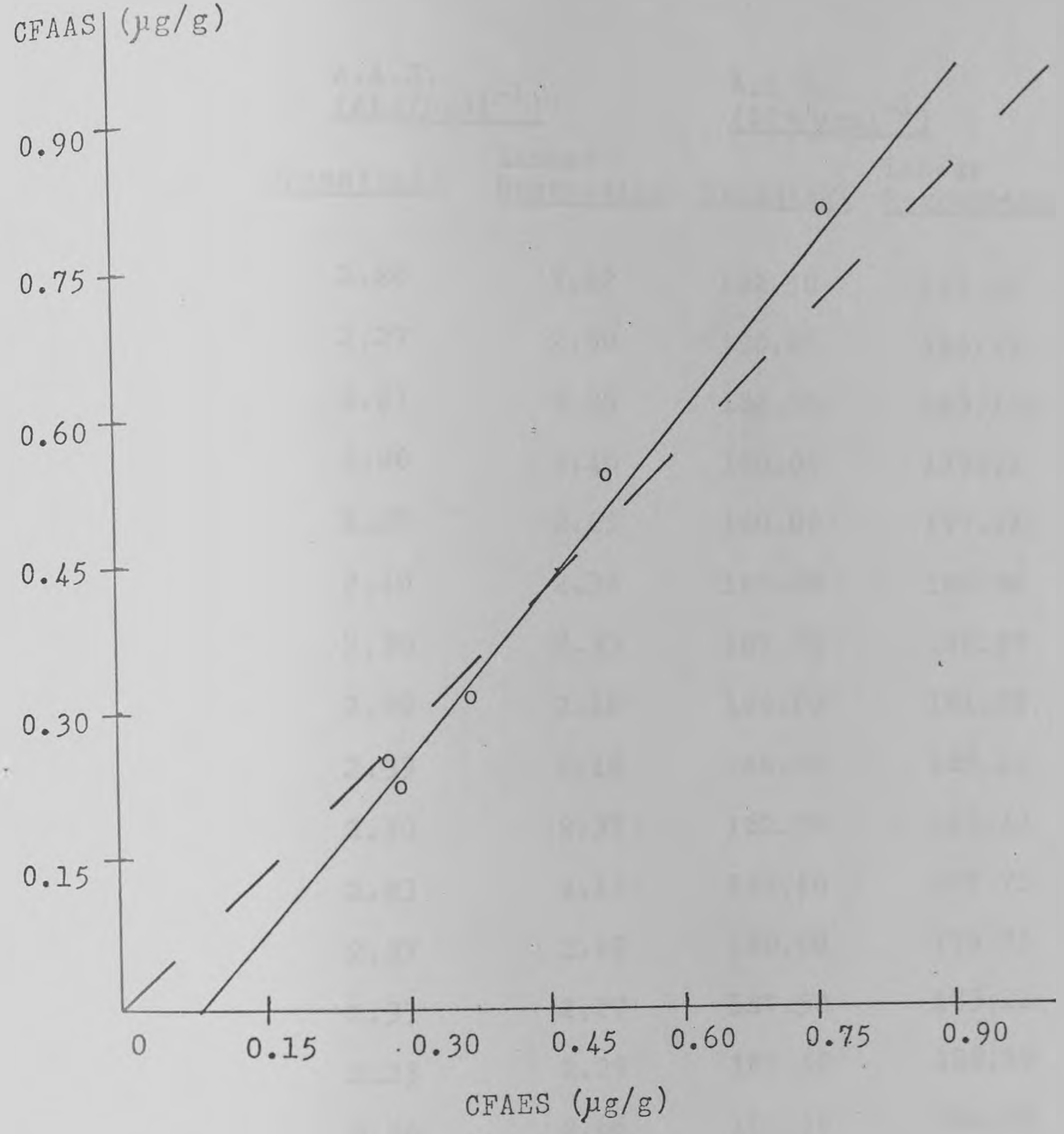

Slope	1.21
Correlation Coefficient	0.9916
Intercept	0.092 µg/g

--- 45° line

—— Linear Regression graph

TABLE 4.3.6

Slopes Calculated from Standard Addition Data for Sphalerite Analysis

	A.A.S. (Abs/µgml^{-1})		A.E.S. (Div/µgml^{-1})	
Sample No	Graphical	Linear Regression	Graphical	Linear Regression
1	2.20	2.22	182.50	183.43
2	2.27	2.30	190.00	186.29
3	2.27	2.26	182.50	183.43
4	2.20	2.40	180.00	179.71
5	2.27	2.25	180.00	177.14
6	2.40	2.32	180.00	180.86
7	2.30	2.33	187.50	188.57
8	2.20	2.18	180.00	184.29
9	2.33	2.48	180.00	185.43
10	2.30	2.37	182.50	183.42
11	2.23	2.13	187.50	187.71
12	2.37	2.40	180.00	175.71
13	2.33	2.27	187.50	189.14
14	2.23	2.29	187.50	188.29
15	2.56	2.66	182.50	182.00
MEAN	2.30	2.32	183.33	183.68
ACID CALIBRATION	2.31	2.36	183.33	183.68

TABLE 4.3.7

Slopes Calculated from Standard Addition Data for Galena Analysis

	A.A.S. $(Abs/\mu gml^{-1})$		A.E.S. $(Div/\mu gml^{-1})$	
Sample No	Graphical	Linear Regression	Graphical	Linear Regression
1	1.98	1.93	7667	7700
2		-	7833	7900
3		-	7500	7550
4	2.06	2.11	7667	7500
5		-	7833	7500
6		-	7333	7200
7		-	7667	7500
8	2.29	2.36	7667	7600
9	2.24	2.19	7500	7350
10	2.07	2.15	7500	7450
11		-	7667	7500
12		-	7667	7650
13		-	7167	7200
14		-	7667	7600
MEAN	2.13	2.17	7595	7518
ACID CALIBRATION	2.07	2.13	7500	7407

TABLE 4.3.8

Replicate Analysis of Sphalerite And Galena Samples

Atomic Absorption

Sample No	Ore	1	2	3	4	5	$\bar{X}$	SD	RSD%	2σ
1	Sphalerite	34.8	34.1	34.6	35.2	34.1	34.6	0.47	1.4	0.94
13	"	7.6	7.9	8.2	7.2	7.3	7.6	0.42	5.5	0.84
1	Galena	0.13	0.10	0.19	0.21	0.16	0.16	0.044	27.5	0.088
8	"	0.82	0.90	0.89	0.86	0.84	0.86	0.033	3.8	0.066

Atomic Emission

1	Sphalerite	34.1	33.9	33.6	33.2	33.6	33.7	0.34	1.0	0.68
13	"	7.9	7.0	7.1	8.3	8.0	7.7	0.58	7.5	1.16
1	Galena	0.20	0.14	0.16	0.18	0.24	0.18	0.038	21.1	0.076
8	"	0.81	0.80	0.74	0.83	0.82	0.80	0.035	4.4	0.007

significant interferant within the sample matrix.

Replicate analysis of two sphalerite and galena samples was carried out and the results are presented in Table 4.3.8. Five dissolutions were carried out on each sample for analysis by atomic absorption and a further five for analysis by atomic emission. Blanks were obtained along with the samples in both cases and an acid calibration graph was used to obtain the concentration of indium.

4.4 CHART RECORDER SIGNALS

The following figures give examples of typical signals obtained during the course of the studies. Figure 4.4.1 shows the signal reproducibility obtained for both CFAAS and CFAES using a tantalum coated tube under gas stop conditions. The signals were obtained from 0.10µg/ml and 0.05µg/ml indium solutions for CFAAS and CFAES respectively. Figure 4.4.2 shows the effect of interference by nitric and hydrochloric acid on a 0.20µg/ml indium solution using CFAAS with a tantalum coated tube Figures 4.4.3 and 4.4.4 show the signals obtained from acid calibration solutions and three sample solutions for galena and sphalerite. The signals were obtained by CFAES using a tantalum coated tube for sphalerite and a tantalum platform in conjunction with a tantalum coated tube for galena.

Figure 4.4.1 Reproducibility of Aqueous Standards Using CFAAS and CFAES

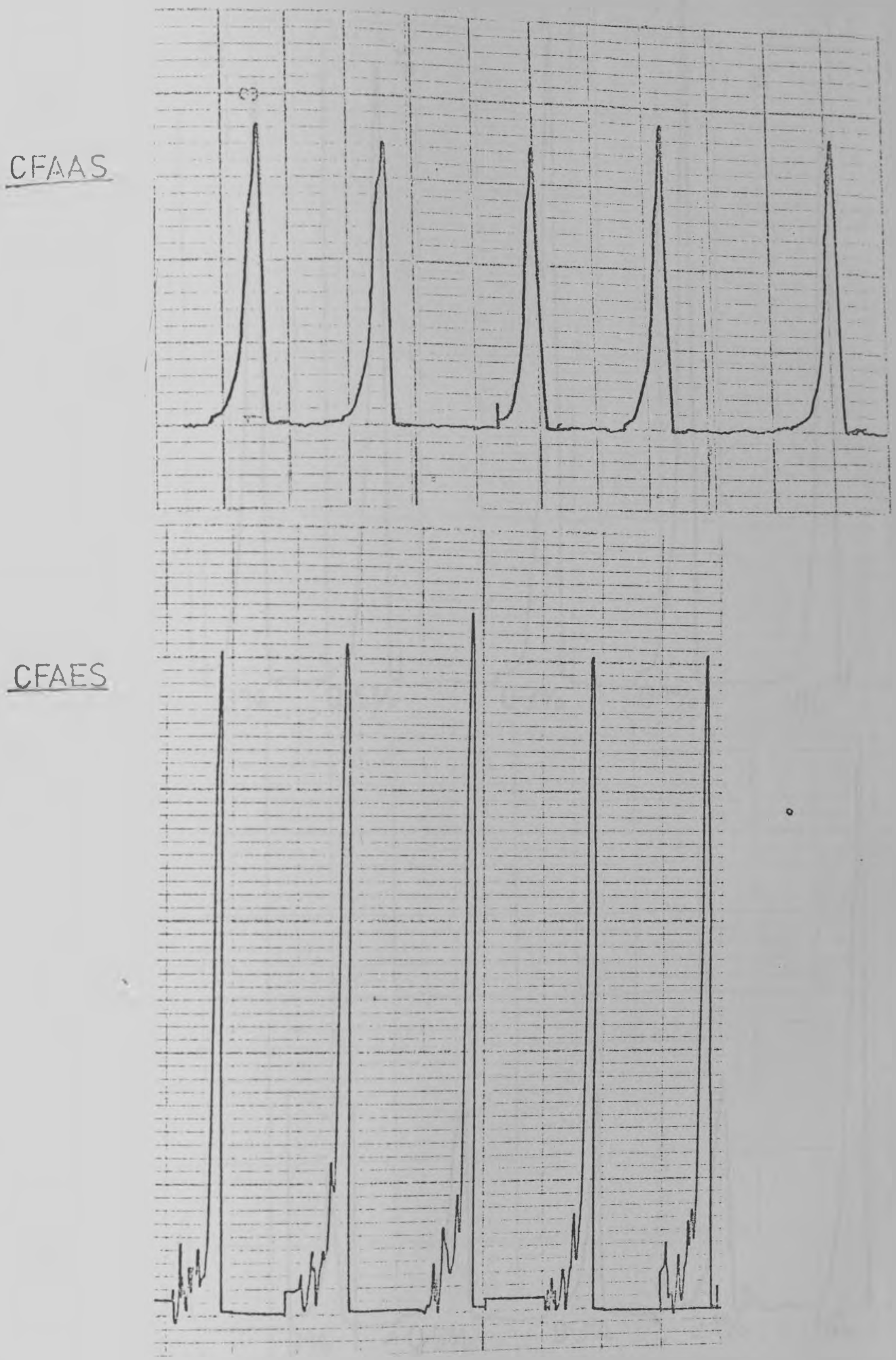

Figure 4.4.2 Interference by HNO_3 and HCl on the Indium signal using CFAAS

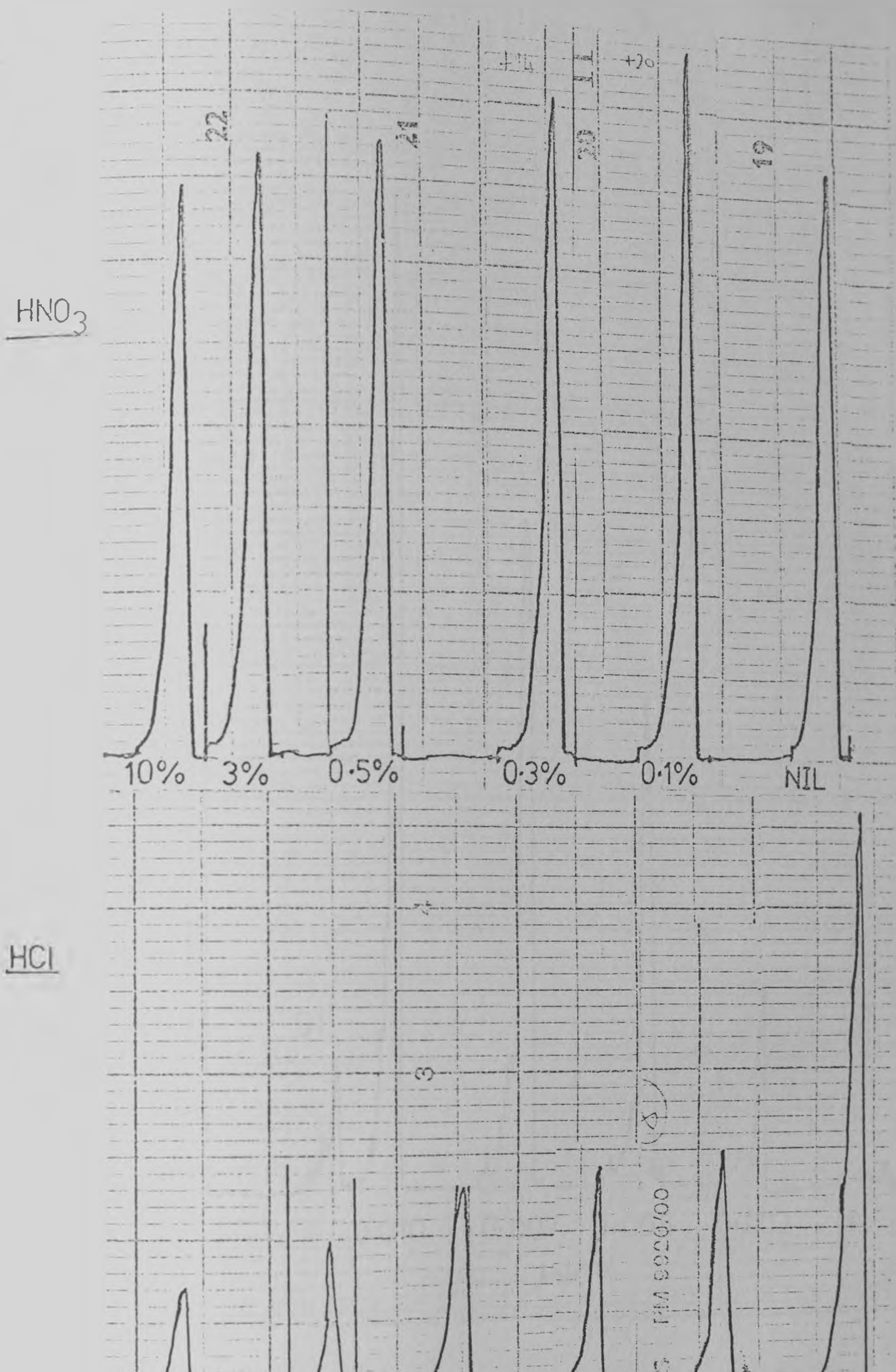

Figure 4.4.3 Galena Analysis using CFAES

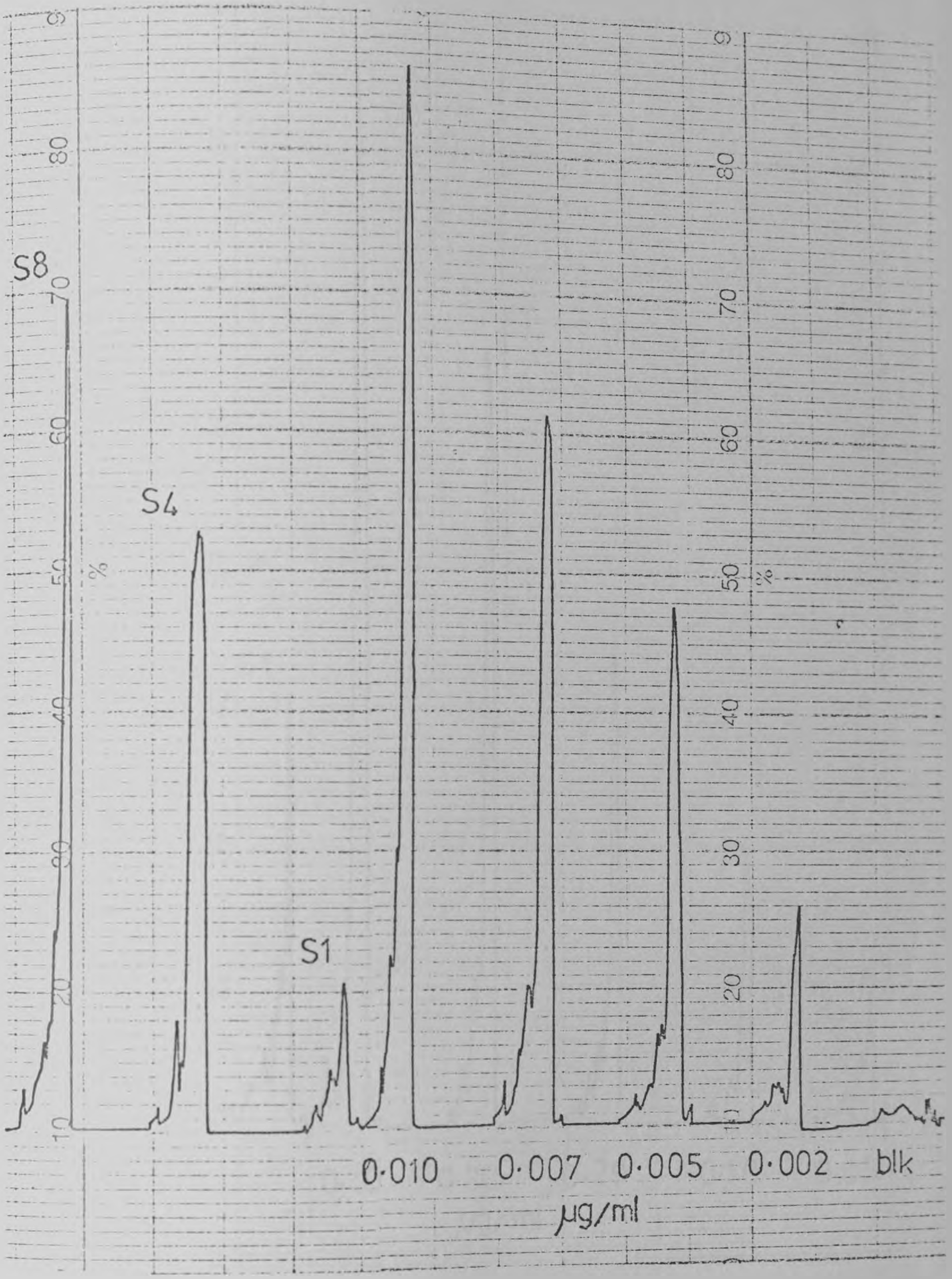

Figure 4.4.4 Sphalerite Analysis using CFAES

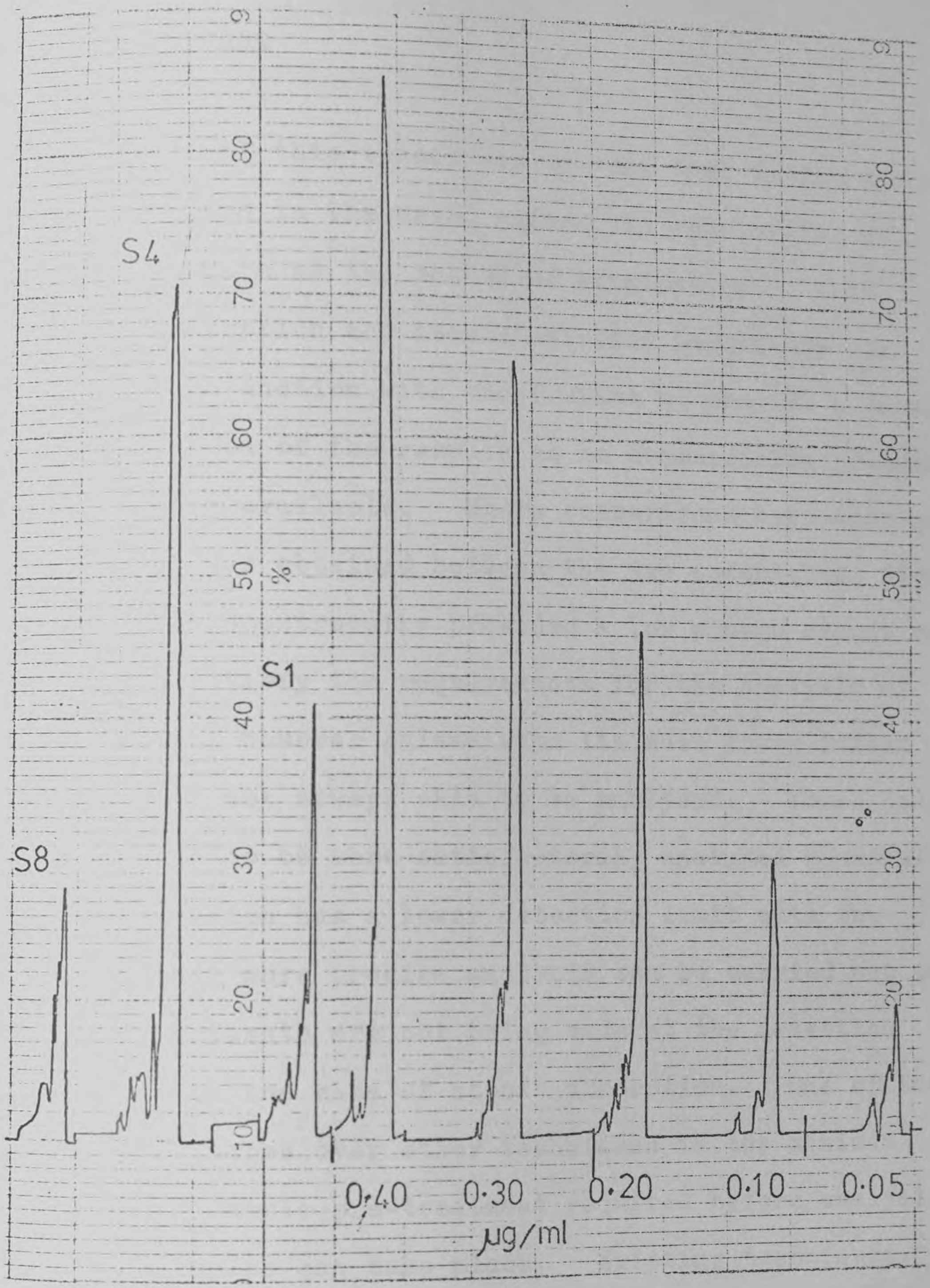

CHAPTER FIVE

CONCLUSIONS

5.1 Resume

The object of this thesis was to show that indium could be determined in the ores, galena and sphalerite, with a carbon furnace as the method of atomisation. Both atomic absorption and atomic emission techniques were used in conjunction with the furnace to provide a means of comparison of the results as no commercially produced standard is available. Where comparisons were made good agreement was obtained between the two techniques. Atomic absorption spectrometry provides a low enough detection limit to satisfy the requirements for the analysis of sphalerite, however galena with its much lower indium content is not always able to be analysed. These samples were found to be more satisfactorily analysed by atomic emission which has a lower detection limit with the result that more precise analysis can be carried out as the measurements are not being made at the detection limit as in the case of atomic absorption. One of the main advantages over other techniques is the minimum amount of sample pre-treatment required before analysis of the samples can take place. Existing techniques often require complicated chemical manipulation including solvent extraction or ion exchange to either remove interferences or to concentrate the indium before analysis but here no such complications are required. It can therefore be stated with some confidence that carbon furnace atomisation allied to atomic absorption and atomic emission provides an accurate method for the determination of indium in these two media.

The use of platform atomisation gives the analyst the opportunity for the reduction of the detection limit without resorting to more expensive equipment. The platforms are cheap and easy to construct and allow atomisation to take place when the conditions in the tube are closer to being isothermal. For the future the use of a probe offers the possibility of another step forward. Here the tube is heated to the atomisation temperature for approximately ten seconds before the probe is introduced resulting in isothermal conditions in the tube.

The tantalum coating procedure adopted also proved to be very useful in that the lifetime of the tube could be greatly extended. The resistance to acid attack was important in this analysis with the acid media used for sample dissolution. The normal tube quickly deteriorated especially with the use of nitric and sulphuric acids and standards required to be run frequently. The tantalum tube however gave a steady signal response even after 200-300 firings.

The use of the atomic emission system can claim to give detection limits which are comparable or better than any other analytical technique. The lack of a commercially available instrument however will restrict the development of this method. This type of system is ideally suited to elucidating many geological problems involving the origin and distribution of trace elements and it is to be hoped that in the future geologists will make more use of both these methods of analysis.

REFERENCES

1. M. J. Russell, Trans. Inst. Mining and Metallurgy, 1974, 83, , B65.

2. T. B. Pierce, P. F. Peck, Ibid, 1961, 86, 580.

3. O. Johansen, E. Steinnes, Talanta, 1966, 13, 1177.

4. G. M. Eskenazy, E.I. Mincheva, Analyst, 1978, 103, 1179.

5. D. M. Shaw, Geochimica et Cosmochimica Acta, 1952, 2, 185.

6. S. R. Taylor, Geochimica et Cosmochimica Acta, 1965, 29, 1243.

7. W. Wahler, J. B. Nenes, Miner. Abh. 1968, 108(1), 36.

8. V. V. Ivanov, Geokhimiya, 1963, 12, 1101.

9. D. M. Shaw, Geochimica et Cosmochimica Acta, 1954, 3, 268.

10. V. M. Goldschmidt, Skr. Norske Vid.-Acad. Oslo, 1937, 1. Mat.-Naturv. Klasse, No. 4.

11. O. Erametsa, Ann.Acad. Sci. Fennicae. Ser., 1938, 1, 50.

12. J. Ottemann, Z. Angew. Mineral, 1940, 3, 142.

13. E. M. Shazly, Trans. Inst. Mining and Metallurgy, 1952, 3, 241.

14. D. C. Greig, The South of Scotland 3rd Edition British Regional Geology, 1971.

15. E. K. Walton, The British Caledonides, 1963, 71.

16. G. V. Wilson, J. S. Flett, Special Report Mineral Resources of Great Britain, 1921, 17.

17. A. K. Temple, Trans. of the Royal Society of Edinburgh, 1955, 63, 85.

18. P. R. Ineson, J. G. Mitchell, Trans. Inst. Mining and Metallurgy, 1969, 78, 29.

19. R. C. L. Larter, A. J. Boyce, M. J. Russell, Mineral Deposita, 1981, 16, 309.

20. M. J. Russell, M. Solomon, J. L Walshe, Mineral Deposita, 1981, 16, 113.

21. F. J. Sawkins, Economic Geology, 1966, 61, 385.

22. A. S. King, Astrophysics Journal, 1905, 21, 236.

23. S. L. Manelshtam, N. N. Semenov, Z. M. Turtovseva, Zhur. Analit. Khim. 1956, 11, 9.

24. B. V. L'vov, Journal Eng. Physics, (U.S.S.R.) 1959, 2, 44.

25. H. Massmann, Z. Analyte. Chem, 1967, 225, 203.

26. H. Massmann, Spectrochimica Acta, 1968, 23B, 215.

27. R. Woodriff, G. Ramelow, Spectrochimica Acta, 1968, 23B, 665.

28. T. S. West, X. R. Williams, Analytica Chimica Acta, 1969, 45, 23.

29. H. M. Donega, T. E. Burgess, Analytical Chemistry, 1970, 42, 1521.

30. J. Aggett, A. J. Sprott, Analytica Chimica Acta, 1974, 72, 49.

31. W. C. Campbell, J. M.Ottaway, Talanta, 1974, 21, 837.

32. R. E. Sturgeon, C. L. Chakrabarti, C. H. Langford, Analytical Chemistry, 1976, 48, 1792.

33. L. de Galan, XX C.S.I./7th I.C.A.S. Prague, 1977.

34. L. de Galan, W.M.G.T. Van den Broek, Analytical Chemistry, 1977, 49, 2176.

35. B. V. L'vov, Atomic Absorption Spectrochemical Analysis, Adam Hilger, London 1970.

36. C. W. Fuller, Analyst, 1974, 99, 739.

37. S. Akman, O.Genc, T. Balkis, Spectrochimica Acta, 1981, 36B, 1121.

38. S. Akman, O. Genc, A. R. Ozdural, T. Balkis, Spectrochimica Acta, 1980, 35B, 373.

39. B. V. L'vov, Spectrochimica Acta, 1978, 33B, 153.

40. R. E. Sturgeon, C. L. Chakrabarti, Analytical Chemistry, 1977, 49, 1100.

41. M. L. Kaiser, S. R. Koirtyohann, . J. Hindenberger, Spectrochimica, Acta, 1981, 36B, 773.

42. V. J. Zatka, Analytical Chemistry, 1978, 50, 538.

43. D. Littlejohn, J. M. Ottaway, Analyst, 1977, <u>102</u>, 553.

44. R. E. Sturgeon, C. L. Chakrabarti, Spectrochimica Acta, 1977, <u>32B</u>, 231.

45. W. M. G. T. Van den Broek, L. de Galan, L. Matousek, E. J. Czobik, Analytica Chimica Acta, 1978, <u>100</u>, 121.

46. J. F. Alder, A. J. Samuel, R. D. Snook, Spectrochimica Acta, 1976, <u>31B</u>, 509.

47. D. Littlejohn, J. M. Ottaway, Analyst, 1979, <u>104</u>, 208.

48. J. M. Ottaway, L. Bezur, J. Marshall, Analyst, 1980, <u>105</u>, 1130.

49. J. M. Ottaway, L. Bezur, R. Fakhrul-Aldeen, W. Frech, J. Marshall, Trace Element Analytical Chemistry in Medicine and Biology, 1980.

50. I. Martinsen, F. J. Langmyhr, Analytica Chimica Acta, 1982, <u>135</u>, 137.